Ana Ribeiro

3-Bromopyruvate as an anticancer agent in breast cancer cell lines: exploring the role of monocarboxylate transporters

Uminho | 2013

Universidade do Minho
Escola de Ciências

Ana Luísa Ferreira Ribeiro

3-Bromopyruvate as an anticancer agent in breast cancer cell lines: exploring the role of monocarboxylate transporters

Mestrado em Genética Molecular

Trabalho realizado sob a orientação de:
Professora Doutora Margarida Casal
Professora Doutora Ana Preto

Outubro de 2013

Universidade do Minho
Escola de Ciências

Ana Luísa Ferreira Ribeiro

3-Bromopyruvate as an anticancer agent in breast cancer cell lines: exploring the role of monocarboxylate transporters

Mestrado em Genética Molecular

Trabalho realizado sob a orientação de:
Professora Doutora Margarida Casal
Professora Doutora Ana Preto

Outubro de 2013

DECLARAÇÃO

Nome: Ana Luísa Ferreira Ribeiro

Endereço electrónico: ribeiro.aluisa@gmail.com

Nº do Bilhete de Identidade: 13539435

Título da Dissertação de Mestrado:

3-Bromopyruvate as an anticancer agent in breast cancer cell lines: exploring the role of monocarboxylate transporters

Orientadores:

Professora Doutora Margarida Casal

Professora Doutora Ana Preto

Instituição de Acolhimento:

Centro de Biologia Molecular e Ambiental (CBMA)

Ano de Conclusão: 2013

Designação do Mestrado:

Mestrado em Genética Molecular

Universidade do Minho, 31 de Outubro de 2013

_____

Ana Luísa Ferreira Ribeiro

Agradecimentos

Expresso a minha gratidão a todas as pessoas que, direta ou inderetamente, contribuiram para a concretização deste trabalho. Gostaria de registar o meu sincero agradecimento:

Às minhas orientadoras, Professora Doutora Margarida Casal e Professora Doutora Ana Preto, pela oportunidade única de desenvolver este trabalho nos seus grupos de investigação. Pela orientação, partilha do rigor científico, disponibilidade e ensinamentos transmitidos. Quero agradecer ainda a revisão crítica desta dissertação. O meu muito obrigada por tudo.

Ao João, por toda a disponibilidade, paciência e sugestões diárias na realização do trabalho experimental. Quero ainda agradecer a leitura e crítica desta dissertação. Muito obrigada pela preciosa ajuda durante todo este ano de trabalho.

À Professora Doutora Fátima Baltazar, à Doutora Céline Pinheiro e à Dra. Filipa Santos, pela constante disponibilidade. Muito obrigada.

A todos os meus colegas dos laboratórios de Biotecnologia Molecular e Biologia Animal, pelo excelente ambiente de trabalho, momentos de boa disposição e ensinamentos. Um obrigada para o Raul, André, Mário, Margarida, Joana, Telma e Pedro do LBM e para a Lisandra, Eugénia, Cristina, Carla, Dalila, Ana Luísa, Joana, Rogério, Filipa, Odete e Teresa do LBA. Um agradecimento muito especial à Suellen por toda a disponibilidade, ensinamentos transmitidos e todo o cuidado. Ao Artur Ribeiro, pela disponibilidade e dicas para a realização deste trabalho.

A todos os Professores, investigadores e funcionários do Departamento de Biologia pela disponibilidade em qualquer situação. Muito obrigada.

A todos os meus amigos por estarem sempre presentes. Muito obrigada Paula, Marina, Claúdia, David, Rafael, Hugo e Ângela.

A toda a minha Família pelos valores transmitidos, em especial aos meus pais pelo amor, incentivo, orientação e acima de tudo por acreditarem sempre em mim. A eles dedico este trabalho.

3-Bromopyruvate as an anticancer agent in breast cancer cell lines: exploring the role of monocarboxylate transporters

Abstract

The development of a tumor is marked by several metabolic alterations mainly at the glycolytic level. The Warburg effect is reflected into the ability of tumor cells to produce most of their energy from glycolysis even in the presence of oxygen (aerobic glycolysis), leading to an increased production of lactate. The monocarboxylate transporters (MCTs) play a central role in maintenance of high glycolytic rates allowing the efflux of lactate to extracellular environment, which contribute to acidic microenvironment important in the maintenance and tumor progression. The pyruvate analogue, 3-bromopyruvate (3-BP), whose transport can be mediated by MCTs, is an alkylating agent able to inhibit the action of metabolic enzymes, leading to ATP depletion and consequent cell death. In a previous work, our group demonstrated that pre-incubation of breast cancer cell lines with butyrate increased the cytotoxic effect of 3-BP, especially in the ones more resistant to 3-BP, by inducing localization of MCT1 in the plasma membrane, as well as upregulation of MCT4 expression. In the present study, we aimed to characterize the effect of butyrate alone or in simultaneous with 3-BP, in four breast cancer cell lines with different sensibilities to 3-BP and evaluated the expression of MCTs in these conditions.

Our results showed that the four human breast cancer cell lines, namely two luminal subtype (ZR-75-1 and MCF-7), one basal subtype (MDA-MB-231) and one HER^{2+} subtype (SK-BR-3) presented a distinct basal expression pattern of MCTs. Butyrate induced cell death dependent on its concentration and also increased the expression of MCT4 but not MCT1, more evident in the cell lines more sensitive, namely ZR-75-1 and MCF-7. Regarding the simultaneous treatment, the presence of low dose of butyrate contributed to cytotoxic effect of 3-BP, while the high dose led to an inhibition effect in the ZR-75-1 and MCF-7 cell lines. These results were correlated with increased expression of MCT2 in these conditions. Higher dose of butyrate alone or in combination with 3-BP, increased the number of cells in G1-phase of the cell cycle in the cell line MDA-MB-231, sensitizing cells to the cytotoxic effect of 3-BP. Moreover, we observed that 3-BP reduced the amount of actin in ZR-75-1. In order to understand the role of MCTs in response to 3-BP we started the optimization of the conditions for siRNA-mediated silencing of MCT1 and MCT4 in ZR-75-1, MCF-7 and SK-BR-3 cell lines. The results obtained in this study intend to contribute towards a better understanding of molecular mechanisms of the 3-BP action, and open novel therapeutic possibilities for breast cancer.

3-Bromopiruvato como agente anticancerígeno em linhas celulares de cancro da mama: explorando o papel dos transportadores de monocarboxilatos

Resumo

O desenvolvimento do tumor é marcado por alterações metabólicas principalmente ao nível da glicólise. O efeito de Warburg traduz-se na capacidade das células tumorais produzirem a maior parte da sua energia a partir da glicólise mesmo na presença de oxigénio (glicólise aeróbica), levando à produção aumentada de lactato. Os transportadores de monocarboxilatos (MCTs) desempenham um papel central na manutenção da elevada taxa glicolítica permitindo o efluxo do lactato para o meio extracelular, que contribui para o microambiente acídico importante na manutenção e progressão do tumor. O análogo do piruvato, 3-Bromopiruvato (3-BP), cujo transporte pode ser mediado por MCTs, é um agente alquilante capaz de inibir a ação de enzimas metabólicas, levando à depleção de ATP e consequente morte celular. Num trabalho anterior, o nosso grupo demonstrou que em linhas celulares de cancro da mama a pré-incubação com butirato aumentou o efeito citotóxico do 3-BP, especialmente na linha celular mais resistente, induzindo a localização do MCT1 na membrana plasmática, assim como um aumento da expressão do MCT4. No presente estudo, procurou-se caracterizar o efeito do butirato aplicado sem ou com o 3-BP em simultâneo, em quatro linhas celulares de cancro da mama com diferentes sensibilidades para o 3-BP, e avaliar a expressão dos MCTs nestas condições.

Os resultados mostraram que as quatro linhas celulares humanas de cancro da mama, nomeadamente duas subtipo luminal (ZR-75-1 e MCF-7), uma subtipo basal (MDA-MB-231) e uma subtipo HER^{2+} (SK-BR-3), apresentaram um padrão de expressão basal de MCTs muito distinto. O butirato induziu morte celular dependente da concentração, e também aumentou a expressão do MCT4, mas não do MCT1, mais evidente nas linhas celulares mais sensíveis, nomeadamente ZR-75-1 e MCF-7. Relativamente ao tratamento simultâneo, a baixa dose de butirato contribuiu para o efeito citotóxico do 3-BP, enquanto que a elevada dose levou a uma inibição do seu efeito nas linhas celulares ZR-75-1 e MCF-7. Estes resultados foram correlacionados com o aumento da expressão do MCT2 nestas condições. A elevada dose de butirato, aplicado sozinho ou em combinação com o 3-BP, induziu um aumento do número de células em fase G1 do ciclo celular na linha celular MDA-MB-231, sensibilizando as células para o efeito do 3-BP. Além disso, observou-se que o 3-BP reduziu a quantidade de actina nas ZR-75-1. A fim de compreender o papel dos MCTs na resposta ao 3-BP foram optimizadas as condições para o silenciamento mediado por siRNA do MCT1 e MCT4 nas linhas celulares ZR-75-1, MCF-7 e SK-BR-3. Os resultados obtidos neste estudo pretendem contribuir para uma melhor compreensão dos mecanismos moleculares de ação do 3-BP, e abrir novas possibilidades terapêuticas para o cancro da mama.

Index

Abbreviations

3-BP - 3-bromopyruvate

5-FU - 5-fluorouracil

^{18}FDG-PET - [^{18}F]-fluorodeoxyglucose positron emission tomography

ACL - ATP citrate lyase

AE1 - Anion exchanger 1

AGO2 - Argonaute 2

AIF - Apoptosis-inducing factor

Akt - Protein kinase B

AMP - Cyclic adenosine monophosphate

AMPK - AMP-activated protein kinase

APS - Ammonium persulfate

Ara-C - Cytarabine

ATCC - American Type Culture Collection

ATP - Adenosine triphosphate

BCA - Bicinchoninic acid

Bcl-2 - B-cell CCL/lymphoma 2

BSA - Bovine serum albumin

BRCA1 - Breast cancer 1 gene

BRCA2 - Breast cancer 2 gene

BRAF - V-raf murine sarcoma viral oncogene homolog B

CA9 - Carbonic anhydrase 9

CG - Core glycosylated

CHC - α-cyano-4-hydroxycinnamate

COX - Cytochrome *c* oxidase

CPE - Choroid plexus epithelia

DAPI - 4',6-Diamidino-2-Phenylindole

DCA - Dichloroacetate

DIDS - 4,4'-diisothiocyanostilbene-2,2'-disulphonate

DNA - Deoxyribonucleic acid

EDTA - Ethylenediaminetetraacetic acid

EMMPRIN - Extracellular Matrix Metalloproteinase Inducer

ER - Estrogen receptor

FBS - Fetal bovine serum

FDG - 2-(^{18}F)-fluoro-2-deoxy-D-glucose

FG - Fully glycosylated

G6P - Glucose-6-phosphate

G6PD - Glucose-6-phosphate dehydrogenase

GAPDH - Glyceraldehyde-3-phosphate dehydrogenase

GLUT - Glucose transporter

HATs - Histone acetyltransferases

HCl - Hydrochloric acid

HDAC - Histone deacetylase

HER-2 - Human epidermal growth factor receptor-2

HIF - Hypoxia inducible factor

HIF-1 - Hypoxia inducible factor-1

HK II - Hexokinase II

IC_{50} - Half maximal inhibitory concentration

IGF-1 - Insulin like growth factor 1

LDHA - Lactate dehydrogenase isoform A

MCTs - Monocarboxylate transporters

MDBK - Madin Darby Bovine Kidney cells

MMP - Matrix metalloproteinases

mRNA - Messenger RNA

mTOR - Mammalian target of rapamycin

NADH - Nicotinamide adenine dinucleotide reduced

NADPH - Nicotinamide adenine dinucleotide phosphate

NF-κB - Nuclear factor kappa-light-chain-enhancer of activated B cells

NHE - Na^+/H^+ exchanger

NMR - Nuclear magnetic resonance

NPPB - 5-nitro-2-(3-phenyl-propylamino)-benzoate

OMM - Outer mitochondrial membrane

Opti-MEM - Reduced serum medium

OXPHOS - Oxidative phosphorylation

pCMBS - p-chloromercuribenzene sulphonate

PBS - Phosphate-buffer saline

PBS-T - Phosphate-buffer saline tween-20

PDH - Pyruvate dehydrogenase

PDK1 - Pyruvate dehydrogenase kinase 1

PEP - Phosphoenolpyruvate

PET - Positron emission tomography

PFA - Paraformaldehyde

PFK-1 - Phospho-fructokinase-1

PGK - 3-phosphoglycerate kinase

PI - Propidium iodide

Pi - Inorganic phosphate

PI3K - Phosphatidylinositol 3-kinase

PIP3 - Phosphatidylinositol-3,4,5-triphosphate

PK - Pyruvate kinase

PPP - Pentose phosphate pathway

PR - Progesterone receptor

PTEN - Phosphatase and tensin homolog

PVDF - Polyvinylidene difluoride

RAS - Rat sarcoma viral oncogene homolog

Rib-5-P - Ribose-5-phosphate

RISC - RNA-induced silencing complex

RNA - Ribonucleic acid

RNAi - RNA interference

ROS - Reactive oxygen species

RPE - Retinal pigment epithelium

rpm - Rotation per minute

RPMI - Roswell Park Memorial Institute

SCFA - Short-chain fatty acid

SCO2 - Cytochrome c oxidase 2

SDS - Sodium dodecyl sulphate

SEM - Standard error of the mean

SERCA - Sarco/endoplasmic reticulum calcium Ca^{2+}- ATPase

siRNA - Small interfering RNA

siRNA-AF - siRNA non-target labeled with Alexa Fluor

SLC16 - Solute Carrier Family 16

SMCTs - Sodium-linked monocarboxylate transporters

T3 - Triiodothyronine

T4 - Thyroxine

T25 flasks - 25 cm^2 polystyrene culture flasks

TCA (cycle) - Tricarboxylic acid cycle

TDLUs - Terminal ductal lobular units

TEMED - N,N,N',N'-tetramethyl-ethylene-1,2-diamine

TIGAR - TP53-induced glycolysis and apoptosis regulator

TMDs - Transmembrane domains

TSA - Trichostatin A

TUNEL - Terminal dUTP Nick-End Labeling

V-ATPase - Vacuolar-type H^+-ATPase

VDAC - Voltage Dependent Anion Channel

VEGF - Vascular endothelial growth factor

Index of Figures

Index of Tables

1. Introduction

1.1. Hallmarks of cancer

Normal cells from living organisms establish a network that allows them to function, proliferate and die in a balanced environment. Several factors can contribute to the imbalance of the system such as alterations in environmental factors (e.g. radiation, chemical) and accumulation of genetic mutations in somatic cells (Pharoah, Dunning et al. 2004). These alterations can induce damage in DNA that can escape to the DNA repair mechanisms and lead to mutations and possibly disease. Neoplasia results from an uncontrolled cell proliferation that depends on the capability of malignant cells to invade surrounding tissues or metastasize to distant areas of the body (Hanahan and Weinberg 2000).

Carcinogenesis is a multifactorial and a multistep process that requires the acquisition of many biological capabilities in evolution of a normal cell to a malignant state (Hanahan and Weinberg 2000). Most of the alterations observed during carcinogenesis have been postulated as hallmarks of cancer and comprise alterations at molecular, biochemical and functional level. These alterations result in a particular cellular behavior that allow cancer cells limitless replicative potential, which results in an exponential growth by activation of telomerase; capacity to escape programmed cell death; sustained proliferative signaling by activation of oncogenes such as *RAS* and *BRAF* genes; insensitivity to growth-inhibitory signals by inactivation of tumor suppressor genes, such as *p53*, and activation of invasion/metastasis by loss of E-cadherin (Hanahan and Weinberg 2000). Moreover, cancer cells can induce angiogenesis leading to the formation of new blood vessels from an avascular system in a tumor cell mass induced by vascular endothelial growth factor (VEGF). Neovascularization is essential to cancer cells survival allowing the availability of oxygen and nutrients, as well as the release of cellular residual metabolites and carbon dioxide (Hanahan and Weinberg 2000).

Recently were proposed new hallmarks important for carcinogenesis, such as the inflammatory microenvironment, genome instability leading to increase the genetic alterations, the ability to escape immune system and the reprogramming of cellular energy metabolism (Hanahan and Weinberg 2011) (Figure 1). The first two new capabilities, referred as enabling characteristics, contribute to tumor progression by the accumulation of mutations and by inducing an inflammatory response. Finally, the last two capabilities named emerging hallmarks have received some attention given the importance of cancer cell metabolism in proliferation and tumor progression (Hanahan and Weinberg 2011).

The interaction of each one of the ten hallmarks in the tumor context provides favorable conditions to accelerate tumorigenesis by promoting proliferation, progression and resistance to defense mechanisms and, therefore leading to a malignant phenotype.

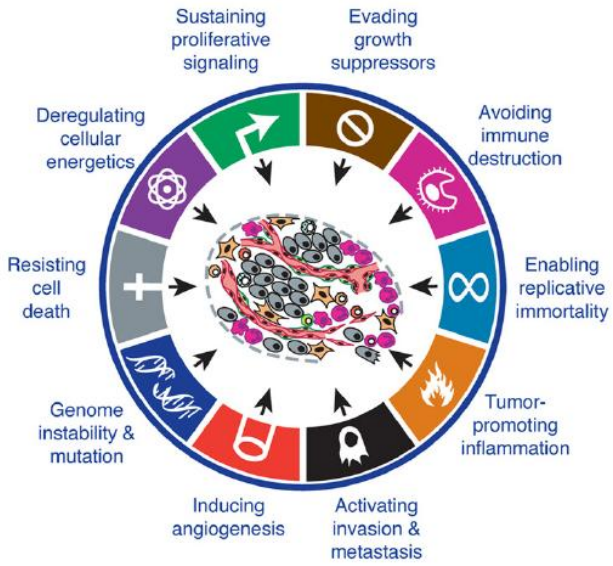

Figure 1. Integrative view of the ten hallmarks of cancer (Hanahan and Weinberg 2011).

1.2. Reprogramming the energy metabolism in cancer cells

Similar to normal cells the metabolism of cancer cells is essential for cell maintenance and proliferation (Vander Heiden, Cantley et al. 2009). Most cancer cells exhibit a peculiar high glycolytic metabolism even in the presence of oxygen which allows adaptation to intermittent hypoxia conditions, higher proliferative rates and resistance to oxidative damages induced by oxidative phosphorylation. Moreover, the end-product of "aerobic glycolysis", lactate is important to create an extracellular acidic environment that favors the maintenance and progression of the tumor cell mass.

1.2.1. Warburg effect in cancer cells

The survival of multicellular organisms requires a constant supply of nutrients. In mammals, cell proliferation is regulated by growth factors that control the uptake of nutrients from the extracellular environment (Vander Heiden, Cantley et al. 2009).

Among all the nutrients, glucose occupies a central position in cell metabolism both as energy source and as a versatile carbon precursor for biosynthetic reactions. Glycolysis, allows the extraction of energy retained in the six-carbon glucose molecule by its oxidation into two three-carbon molecules of pyruvate. In glucose metabolism are involved several enzymes that participate in a series of degradation reactions (catabolic reactions) generating two molecules of NADH (nicotinamide adenine dinucleotide (NAD^+) reduced), two molecules of adenosine triphosphate (ATP) and two molecules of pyruvate per molecule of glucose.

In aerobic conditions, most differentiated tissues acquire cellular energy through the oxidative phosphorylation (OXPHOS), which occurs in the mitochondria (Figure 2). In OXPHOS, pyruvate is completely oxidized to carbon dioxide through the enzymes of the tricarboxylic acid (TCA) cycle associated to maximal ATP production through the respiratory chain in the mitochondria. The free energy resulting from this process is driven to ATP synthasome (ATP Synthase/Pi Carrier/Adenine Nucleotide Carrier complex) to generate ATP from ADP and inorganic phosphate (Pi) in the presence of Mg^{2+}. This process occurs exclusively in aerobic conditions because oxygen is the final electron acceptor of the respiratory chain. In the absence of oxygen (anoxia) or under low oxygen conditions (hypoxia), differentiated cells are unable to support OXPHOS therefore pyruvate is converted to lactate *via* lactate fermentation in the cytosol (Figure 2). In anaerobic metabolism, pyruvate is reduced to lactate by lactate dehydrogenase isoform A (LDHA), accepting electrons from NADH and regenerating NAD^+ needed to maintain glycolysis (Munoz-Pinedo, El Mjiyad et al. 2012). The lactate formed is secreted into the extracellular environment by monocarboxylate transporters (MCTs) (Gatenby and Gillies 2004).

The energetic yield of glucose metabolism *via* OXPHOS generates 36 molecules ATP per molecule glucose, whereas lactate fermentation generates only 2 molecules ATP per molecule glucose (Vander Heiden, Cantley et al. 2009). According to the energetic yield, the presence of adequate oxygen levels inhibits lactate fermentation and the glucose metabolism is driven to OXPHOS which is the process energetically more efficient. This metabolic shift was first demonstrated by Louis Pasteur, who observed in yeast cells reduced fermentation of glucose in the presence of oxygen (Pasteur effect) (Racker 1974).

In contrast to normal differentiated tissues, most cancer cells rely more on glycolysis for ATP production independently on the oxygen availability in the extracellular microenvironment (Figure 2). The high glycolytic rates of cancer cells even in the presence of oxygen was first demonstrated by Otto Warburg (Warburg 1956). The first explanation of this phenomenon termed

Warburg effect or "aerobic glycolysis" was given by him who suggested that irreversible damage in the mitochondrial function in cancer cells limited the oxidative phosphorylation and therefore glucose metabolism occurred exclusively by the glycolytic pathway and it was causally involved in the development of tumors (Warburg 1956). However, it was later found that mitochondrial function is not altered in all cancer cells that exhibits Warburg effect and this would be not the reason for the typical phenotype of cancer cells (Schulze and Harris 2012). Recent studies have shown that glycolytic switch in cancer cells is also promoted by activation of oncogenes as *Ras* and inhibited by tumor suppressor genes, such as *pVHL*, indicating that it is intrinsically associated to carcinogenesis process (Koppenol, Bounds et al. 2011).

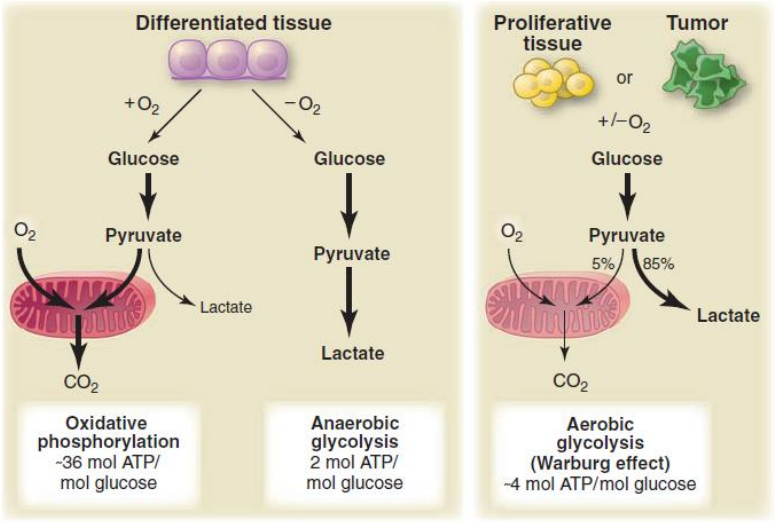

Figure 2. Schematic representation of glucose metabolism in differentiated tissues (left panel), normal proliferative tissues and tumor cells (right panel). In differentiated tissue the presence or absence of oxygen determine two different pathways for glucose metabolism: oxidative phosphorylation and anaerobic glycolysis, respectively. In normal proliferative tissues and tumor cells, glucose metabolism is mainly driven to lactate fermentation even in the presence of oxygen (Warburg effect or aerobic glycolysis) (Vander Heiden, Cantley et al. 2009).

The metabolic reprogramming typical of cancer cells raises many questions: Why cancer cells produce energy by glycolysis under aerobic conditions? What are the advantages of glycolysis for cancer cells? Understanding the role of cell-environment interactions in tumor evolution is the key for these answers.

The hyperproliferative state of cancer cells leads to a development from a normal epithelium to an interstitial neoplasia characterized by uncontrolled cell proliferation that

progresses to a carcinoma *in situ* (Figure 3). In an intratumoral hypoxic environment, cancer cells achieved the oxygen diffusion limit which induces one of the two cell responses: adaptation to anaerobic glycolysis for ATP production which allows cells to survive or cell death. The metabolic adapted cancer cells acquire the ability of motility that leads to basement membrane breakdown and consequent access to blood vessels and lymphatic vasculature progressing the carcinoma *in situ* to an invasive state (Gatenby and Gillies 2004). However, some cancer cells remain glycolytic even oxygen availability is restored in oxygenated regions, producing most of ATP by glycolysis (Mathupala, Colen et al. 2007).

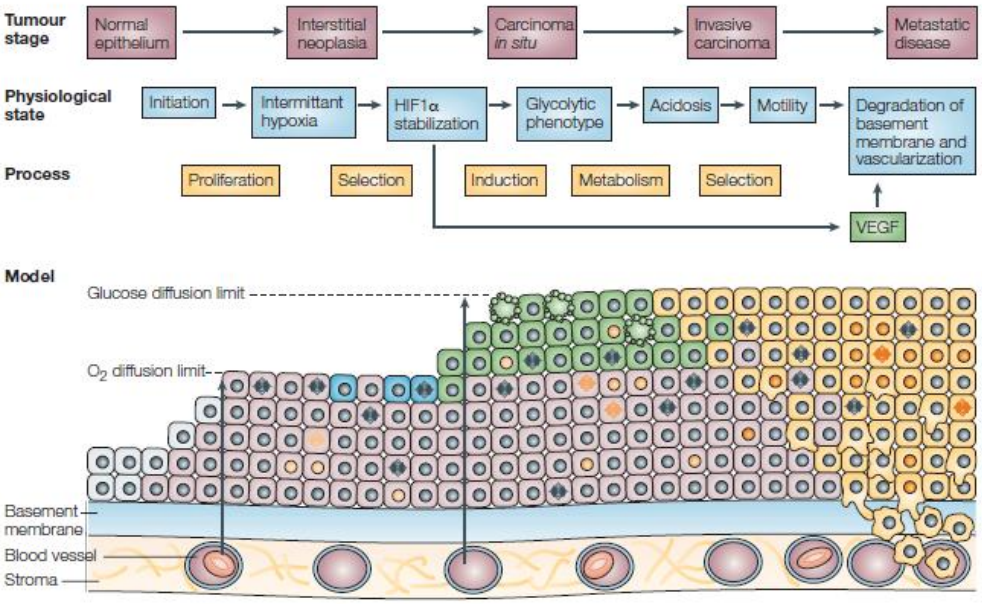

Figure 3. Schematic representation of the cell-microenvironment interactions associated with the carcinogenesis process. Normal epithelial (grey), hyperproliferative (pink), hypoxic (blue), glycolytic (green) and motile cells (yellow) (Gatenby and Gillies 2004).

The rapid proliferation of cancer cells requires cellular energy in form of ATP obtained by glycolysis and supported by high increased of glucose uptake (Vander Heiden, Cantley et al. 2009). The upregulation of glycolysis metabolism generates metabolic intermediates that can be converted into anabolic reactions, such as synthesis of nucleic acids, lipids and proteins, increasing the availability of important biosynthetic precursors for cell growth and proliferation (Figure 4). For instance, the metabolism of glycolytic intermediate glucose-6-phosphate (G6P) through the pentose phosphate pathway (PPP) generates ribose-5-phosphate (Rib-5-P), an important intermediate in nucleotide biosynthesis. The oxidative pathway of PPP can also

produce nicotinamide adenine dinucleotide phosphate (NADPH), which supplies reducing equivalents for both nucleotide and fatty acid biosynthesis (Jones and Thompson 2009). Cancer cells can also take advantage of high glycolytic rates since the lactate efflux creates an extracellular acidic micro-environment which favors the process of invasion/metastasis, by activation of proteases that are involved in degradation of the extracellular matrix and basement membranes, such as metalloproteinases (MMP), (Pedersen 2007; Kroemer and Pouyssegur 2008), activation of proteins as hyaluronan and its receptor CD44, which are molecules involved in invasion and metastization (Stern, Shuster et al. 2002) and also contributes to the evasion from the immune system by blocking the glycolytic pathway of lymphocytes T (Frauwirth and Thompson 2004; Fischer, Hoffmann et al. 2007). Moreover, the exported lactate promotes angiogenesis by increasing vascular endothelial growth factor (VEGF) levels associated with the tumor aggressiveness (Hirschhaeuser, Sattler et al. 2011). On the other hand, the residual rate of OXPHOS metabolism provides protection to DNA damaging induced by reactive oxygen species (ROS) mainly produced in mitochondrial respiratory chain by complex I and III (Kroemer and Pouyssegur 2008). The “aerobic glycolysis” of cancer cells allows the metabolism of glucose in intermittent hypoxia conditions, which is important for the maintaining of the metabolism under different oxygen levels (Lopez-Lazaro 2008).

The interest in the peculiar metabolism of cancer cells led to the discovery of an hexokinase isoform which is overexpressed in cancer cells (Nakashima, Mangan et al. 1986). The enzyme hexokinase II (HK II) catalyzes the formation of glucose-6-phosphate (G6P) from glucose and ATP in the first irreversible step of the glycolysis (Wilson 1995; Wilson 1997). This hexokinase isoform is associated with outer mitochondrial membrane *via* Voltage Dependent Anion Channel Protein (VDAC) allowing both direct access to intramitochondrial ATP synthetized in the ATP synthasome to phosphorylate glucose, and protection from feedback inhibition by its product G6P (Nakashima, Mangan et al. 1986). The interaction of HK II with the complex ATP synthasome also keeps VDAC in the open state which counteracts with outer mitochondrial membrane (OMM) permeabilization involved in intrinsic pathway of apoptosis blocking binding sites for pro-apoptotic Bcl-2 family proteins in the OMM (Gogvadze, Zhivotovsky et al. 2010).

The high increase of glucose uptake by cancer cells is the basis for imaging technique that allows detection of tumors. In this detection system, namely positron emission tomography (PET), is used a glucose analogue tracer ^{18}fluorodeoxyglucose (FDG) which is phosphorylated by hexokinase into a non-metabolizable product that accumulates in highly glycolytic cancer cells.

The accumulation of the radioactive glucose analogue is detected by [^{18}F]-fluorodeoxyglucose positron emission tomography (^{18}FDG-PET) (Gatenby and Gillies 2004). FDG-PET imaging is used as a non-invasive method to cancer diagnosis, as well as to monitor therapeutic response, and also allows the quantification of glucose uptake that is correlated with tumor aggressiveness (Gatenby and Gillies 2004). However, the sensitivity of FDG-PET imaging is lowered for tumors with small size (<0.8 cm^3), and specificity is lowered because immune cells are also capable to trapped FDG (Gatenby and Gillies 2004). Nuclear magnetic resonance (NMR) spectroscopy has been explored as a non-invasive method for the detection of selected metabolites such as glutamine and acetate in tumors *in vivo* and can provide an insight into metabolic response to therapy (Schulze and Harris 2012).

Although glycolysis is the mainly pathway responsible for ATP production in cancer cells, there are other metabolic pathways upregulated, such as glutaminolysis, lipid synthesis, ketone oxidation and serinolysis (Figure 4) (Vander Heiden, Cantley et al. 2009). Glycolysis and glutaminolysis are the most important pathways in the context of tumor. Glutaminolysis is an alternative pathway for ATP production upregulated in MYC-transformed cells (Wise, DeBerardinis et al. 2008). In this pathway, glutamine is converted to glutamate by glutaminase enzyme and generates intermediates of the TCA cycle redirected into biosynthetic reactions important to cell growth and proliferation (Vander Heiden, Cantley et al. 2009).

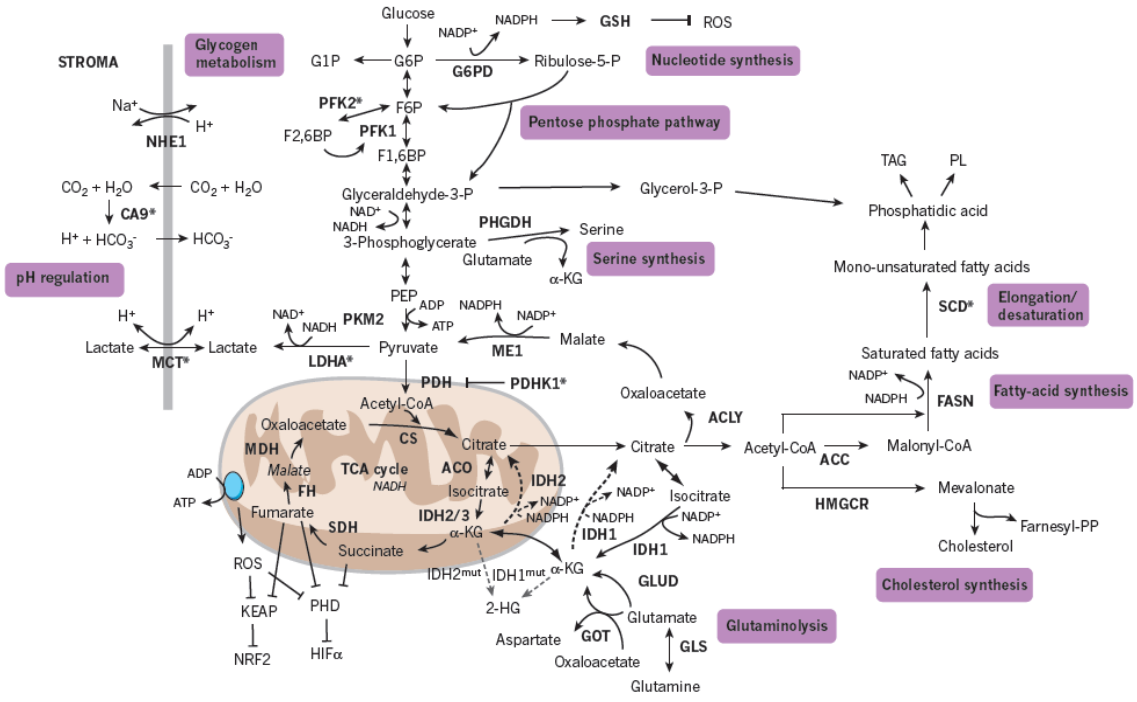

Figure 4. Schematic overview of cancer cells metabolism (Schulze and Harris 2012).

1.2.2. Molecular mechanisms driving Warburg effect

Many of the mutations observed in tumors are related to metabolism control (Figure 5) (Vogelstein and Kinzler 2004). The high glycolytic phenotype of cancer cells can be driven by alterations in signaling pathways that include transcription factors, such as hypoxia inducible factor (HIF) and MYC, and kinases such as mTOR and phosphatidylinositol 3-kinase (PI3K) (Kroemer and Pouyssegur 2008).

A principal regulator of cell metabolism is the PI3K, a lipid kinase that regulates the phosphorylation levels of phosphatidylinositol (PIP3) at the plasma membrane (Jones and Thompson 2009). Activation of PI3K leads to the activation of downstream effectors including mammalian target of rapamycin (mTOR) and the protein kinase B (Akt) that regulate metabolic activities involved in cellular biosynthesis (Jones and Thompson 2009). In normal cells, PI3K activation is high controlled by dephosphorylation of PIP3 by the phosphatase PTEN, a tumor suppressor. The pathway is deregulated in cancer through a diversity of mechanisms, including PTEN loss or activating mutations in PI3K (Jones and Thompson 2009). PI3K/Akt signaling promotes glycolysis through Akt-dependent stimulation by upregulation and membrane localization of glucose transporters (GLUT1 and GLUT4); activity and mitochondrial localization of hexokinase and phosphofructokinase; and enhanced protein translation through Akt-dependent mTOR activation (Edinger and Thompson 2002).

The survival of cancer cells in hypoxia is achieved by activation of the transcription factor hypoxia inducible factor-1 (HIF-1), a heterodimer composed of a constitutive HIF-1β subunit and a labile HIF-1α subunit (Tennant, Duran et al. 2010). Under anoxia conditions, the activation of HIF-1α increases the upregulation of genes involved in glycolysis including glucose transporter 1 and 3 (GLUT 1 and GLUT3), Hexokinase II (HK II, which catalyze the initial step of glycolysis), and lactate dehydrogenase A (LDHA), as well as involved in angiogenesis as VEGF and hematopoietic factors (erythropoietin) that accelerate tumorigenesis (Brahimi-Horn, Chiche et al. 2007; Semenza 2008). HIF1 also promotes the induction of pyruvate dehydrogenase kinase 1 (PDK1), a negative regulator of pyruvate dehydrogenase (PDH) that catalyzes the conversion of pyruvate to acetyl-CoA. This upregulation reduces electron flux through OXPHOS and subsequently reduces oxidative stress resulted from mitochondrial metabolism (Semenza 2008).

Oncogenic c-Myc is a regulator of metabolic pathways essential for tumor progression, such as glycolysis and glutaminolysis (Dang, Kim et al. 2008). MYC promotes aerobic glycolysis

by enhanced the expression of GLUT1 and LDHA (Shim, Dolde et al. 1997). The transcription factor MYC is also important in regulation of proliferation and cell cycle entry (Schulze and Harris 2012).

Inactivation of a tumor suppressor gene *p53* also promotes glycolysis in cancer cells by both decreased a glycolysis inhibitor *TIGAR* (TP53-induced glycolysis and apoptosis regulator) expression, and the synthesis of the protein cytochrome *c* oxidase 2 (SCO2) required for the correct assembly of the cytochrome *c* oxidase (COX) complex of the electron chain in the mitochondria. The loss of p53 protein activity also increases glucose uptake and HIF-1 levels (Vander Heiden, Cantley et al. 2009).

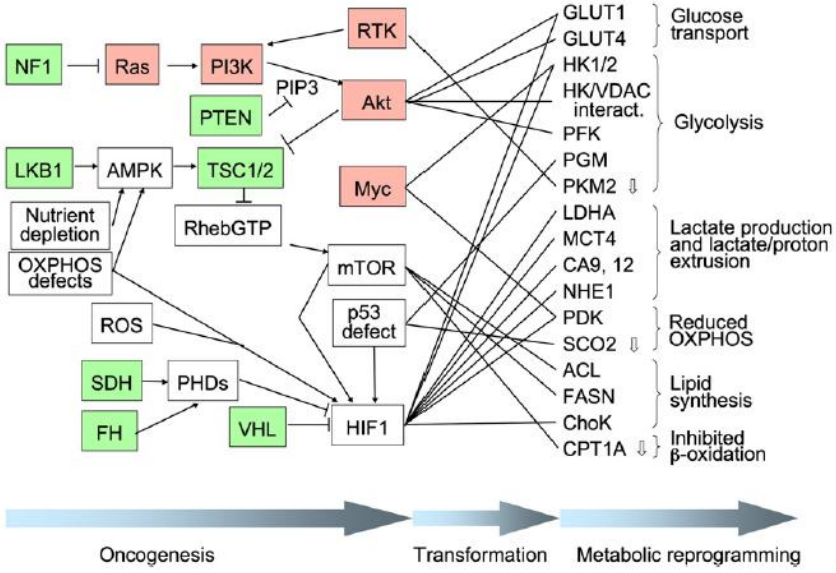

Figure 5. Schematic representation of the molecular mechanisms driven the Warburg effect in cancer cells (Kroemer and Pouyssegur 2008).

1.3. Monocarboxylate transporters

Lactate is the monocarboxylic acid that can be formed as end-product of glycolysis and its intracellular accumulation results in acidification of the cytosol and inhibition of phospho-fructokinase-1 (PFK-1) and consequently glycolysis (Halestrap and Price 1999). Therefore, the transmembrane transport of monocarboxylic acids is an essential mechanism for pH homeostasis in mammalian cells, and is catalyzed by monocarboxylate transporters (MCTs) (Halestrap and Price 1999). The efflux of lactate is particularly important for high glycolytic cells

such as most cancer cells, white and red blood cells, and tissue skeletal muscle (Merezhinskaya and Fishbein 2009).

Actually, are described fourteen human MCT members belonging to the MCTs family encoded by the *SLC16* gene family of solute carriers (Table I) (Halestrap and Meredith 2004; Halestrap and Wilson 2012). The predicted topology of these transporters showed 12 alpha-helical transmembrane domains (TMDs) with an intracellular N- and C-terminus and a large intracellular loop between TMDs 6 and 7 (Poole, Sansom et al. 1996). Based on amino acid sequence and functional similarities, the heterogenic MCTs family can be divided into three main clusters, where MCT1-4 cluster is responsible for the H^+-linked transport of endogenous monocarboxylic acids, such as pyruvate, lactate and ketone bodies across the plasma membrane with different tissue distribution, regulation and substrate/inhibitor affinity (Pinheiro, Longatto-Filho et al. 2012). In MCT1-4 cluster, both influx and efflux of monocarboxylates are cotransporter couple to protons in a equimolar manner by a simport mechanism according to substrate concentration and pH gradient between intracellular and extracellular environment (Halestrap and Wilson 2012). MCTs 5-7, 9 and 11-14 are described as orphan transporters whose substrates are unknown and their functional role is not characterized (Morris and Felmlee 2008). MCT8 and MCT10 have a wide tissue distribution and are thyroid hormones triiodothyronine (T3)/thyroxine (T4) and aromatic aminoacids transporters, respectively. Both MCT8 and MCT10 isoforms have been demonstrated to transport their substrates in a H^+- and Na^+- independent manner (Morris and Felmlee 2008)

Recently has been described two members of Na^+-linked monocarboxylate transporters (SMCTs) solute carrier transporter family, the SLC5A8 (SMCT1) and SLC5A12 (SMCT2) present in the plasma membrane able to transport monocarboxylates across the plasma membrane (Li, Myeroff et al. 2003). SMCTs mediate the active transport of a variety of monocarboxylic acids against its chemical gradient using the energy released by the translocation of Na^+ in favor of its concentration gradient (Miyauchi, Gopal et al. 2004). These transporters demonstrate a more restricted distribution in thyroid gland, kidney, colon, retina and brain, while MCTs show a more ubiquitous distribution (Paroder, Spencer et al. 2006; Ganapathy, Thangaraju et al. 2008; Thangaraju, Cresci et al. 2008). In the intestine SMCT1 transporter mediates the uptake of butyrate from the lumen into colonocytes (Gupta, Martin et al. 2006; Ganapathy, Thangaraju et al. 2008; Thangaraju, Cresci et al. 2008). SMCT1 also function as a tumor suppressor gene in both gliomas and colon cancer (Li, Myeroff et al. 2003).

Table I. The human Monocarboxylate Transporter Family (adapted from Halestrap and Meredith 2004; Morris and Felmlee 2008). T3 – triiodothyronine; T4 – thyroxine; CPE – choroid plexus epithelium; RPE – retinal pigment epithelium

MCT	Human gene name	Substrates	Tissue distribution	Transport mechanism
MCT1	*SLC16A1*	Lactate, pyruvate, ketone bodies	Ubiquitous	H^+ cotransporter exchanger
MCT2	*SLC16A7*	Lactate, pyruvate, ketone bodies	Kidney, brain	H^+ cotransporter
MCT3	*SLC16A8*	Lactate	RPE, CPE	H^+ cotransporter
MCT4	*SLC16A3*	Lactate, pyruvate, ketone bodies	Skeletal muscle, heart, lung, chondrocytes, leucocytes, testis, placenta	H^+ cotransporter
MCT5	*SLC16A4*	Orphan	Brain, muscle, liver, kidney, lung, ovary, placenta, heart	Orphan
MCT6	*SLC16A5*	Orphan	Kidney, muscle, brain, heart, pancreas, prostate, lung, placenta	Facilitated diffusion
MCT7	*SLC16A6*	Orphan	Brain, pancreas, muscle	Orphan
MCT8	*SLC16A2*	T3, T4	Liver, heart, brain, thymus, intestine, ovary, prostate, pancreas, placenta	Orphan
MCT9	*SLC16A9*	Orphan	Endometrium, testis, ovary, breast, brain, kidney, adrenal, RPE	Orphan
MCT10	*SLC16A10*	Aromatic amino acids	Kidney, intestine, muscle, placenta, heart	Facilitated diffusion/exchanger
MCT11	*SLC16A11*	Orphan	Skin, lung, ovary, breast, pancreas, RPE, CPE	Orphan
MCT12	*SLC16A12*	Orphan	Kidney	Orphan
MCT13	*SLC16A13*	Orphan	Breast, bone marrow	Orphan
MCT14	*SLC16A14*	Orphan	Brain, heart, ovary, breast, lung, pancreas, RPE, CPE	Orphan

1.3.1. Function and expression of MCT family

MCT1 has an ubiquitous distribution and catalyzes the cellular uptake and efflux of monocarboxylates such as pyruvate (K_m 0.6-1 mM), L-lactate (K_m 2.2-4.5 mM), proprionate (K_m 1.5 mM), acetate (K_m 3.7 mM), acetoacetate (K_m 5.5 mM), L-β-hydroxybutyrate (K_m 8.1-11.4 mM) and D-β-hydroxybutyrate (K_m 8.1-10.1 mM) (Halestrap and Meredith 2004; Pinheiro, Longatto-Filho et al. 2012). MCT1 is mostly responsible for lactate uptake for oxidation in red skeletal muscles and heart or efflux in glycolytic cells, such as erythrocytes, according to the substrate concentration and pH gradient (Halestrap and Meredith 2004). MCT1 isoform is also associated with the transport of butyrate and proprionate in human colonocytes (Cuff, Lambert et al. 2002). MCT1 function as a proton-dependent cotransporter/exchanger and transport across the membrane occurs by ordered sequential binding with association of a proton followed by lactate binding (Juel and Halestrap 1999). The isoform MCT2 was characterized by heterologous expression in *Xenopus laevis* oocytes and is expressed in gluconeogenic tissues (kidney, liver and brain) where catalyzes with higher affinity the uptake of L-lactate (K_m 0.7 mM), D-β-hydroxybutyrate (K_m 1.2 mM), pyruvate (K_m 0.08 mM) and acetoacetate (K_m 0.8 mM) than MCT1 (Broer, Broer et al. 1999; Pinheiro, Longatto-Filho et al. 2012). MCT3 has a very restricted distribution in the basolateral membrane of the retinal pigment epithelium (RPE) and the choroid plexus epithelia (CPE), and catalyzes the L-lactate export in the retina (Bergersen, Johannsson et al. 1999). Finally, the isoform MCT4 is predominantly expressed in highly glycolytic cells such as white blood cells (leucocytes), white skeletal muscle fibers and astrocytes, exhibiting the highest K_m values for most substrates that MCT1 and MCT3, such as L-lactate (k_m 28.0-34.0) and pyruvate (K_m 153.0) (Dimmer, Friedrich et al. 2000; Pinheiro, Longatto-Filho et al. 2012). The physiologic function of MCT4 is the efflux of lactate of glycolytic cells (Halestrap and Meredith 2004).

Recent studies have shown that MCTs1-4 are heteromeric transporters composed of an catalytic α-subunit (MCT) and an accessory β-subunit (CD147) (Philp, Ochrietor et al. 2003). The expression and functional activity of MCTs1-4 is associated with ancillary proteins that are involved in correct trafficking and anchoring to the plasma membrane. MCT1, 3 and 4 require association with the mature glycosylated form of CD147 protein also known as Extracellular Matrix Metalloproteinase Inducer (EMMPRIN) or basigin (Kirk, Wilson et al. 2000; Gallagher, Castorino et al. 2007; Pinheiro, Reis et al. 2010) in the endoplasmatic reticulum, while MCT2

isoform requires the association with integral membrane glycoprotein gp70 or EMBIGIN (Gallagher, Castorino et al. 2007). MCT4 expression regulates the maturation of CD147 in a high invasive breast cancer cell line MDA-MB-231, supporting the high glycolytic rates and consequent increase in efflux of lactate (Gallagher, Castorino et al. 2007).

1.3.2. Genetic regulation of MCT family

The regulation of MCTs expression can be driven by a variety of stimuli including hormones, exercise and monocarboxylic acids like butyrate and lactate (Kennedy and Dewhirst 2010). MCTs expression undergoes transcriptional, post-transcriptional and post-translational regulation and appears to be regulated in a tissue-specific manner (Morris and Felmlee 2008). Several studies have shown that in skeletal muscle MCT1 levels increase in response to chronic stimulation (e.g. chronic electrical stimulation) or exercise in rats and humans mediated by calcium and cyclic adenosine monophosphate (AMP) that activate calcineurin and AMP-activated protein kinase (AMPK) (Coles, Litt et al. 2004; Halestrap and Wilson 2012). Thyroid-stimulating hormone has also been associated with the upregulation of MCT1 and MCT4 expression in skeletal muscle (Halestrap and Wilson 2012). Treatment with testosterone resulted in an increase of MCT1 protein expression without alteration in MCT1 mRNA level suggesting an post-transcriptional regulation (Enoki, Yoshida et al. 2006). Others studies have shown that butyrate stimulate MCT1 promoter activity in both colon cancer cell line Caco-2 and colonic epithelial cell line AA/C1 *via* NF-κB pathway suggesting a transcriptional regulation mechanism (Cuff, Lambert et al. 2002; Borthakur, Saksena et al. 2008). Recently were suggested that GPR109A, a luminal short-chain fatty acid (SCFA) sensor, mediates the effects of SCFA substrates in MCT1 membrane localization and function (Borthakur, Priyamvada et al. 2012). High concentrations of lactate have been reported to increase MCT1 mRNA and protein levels in L6 myoblasts cells *via* NF-κB pathway (Hashimoto, Hussien et al. 2007). Trichostatin A (TSA), a histone deacetylase (HDAC) inhibitor can also induce the activity of MCT1 promoter in human intestinal epithelial cells (Borthakur, Saksena et al. 2008). Post-translational regulation of MCT1 by microRNAs has also been observed were miR-29a and miR-29b contribute to silence MCT1 expression in pancreatic β-cell-specific (Pullen, da Silva Xavier et al. 2011) and miR-124, a microRNA in the mammalian nervous system, regulates MCT1 expression in medullobastoma cells (Li, Pang et al. 2009). MCT1 gene is reported to be hypermethylated (Hussien and Brooks 2011).

The isoform MCT2 has been reported to be regulated by post-translational mechanisms (Halestrap and Wilson 2012). In brain, MCT2 expression is enhanced by noradrenaline, insulin and insulin like growth factor 1 (IGF-1) by translational activation (Halestrap and Wilson 2012). Obesity has also been associated with the upregulation of MCT2 mRNA expression levels in the brain of a rat OVX+E_2 model (Matsuyama, Ohkura et al. 2009).

MCT4 is mainly upregulated by hypoxia conditions through a HIF-1α-dependent mechanism, which is in accordance with the role of this transporter in lactate export from glycolytic cells (Ullah, Davies et al. 2006). Butyrate has also reported to increase the expression of MCT4 and the localization of MCT1 at the plasma membrane in the human breast cancer cell line SK-BR-3 (Queiros, Preto et al. 2012). MCT4 silencing is achieved by promoter methylation (Huang, Plass et al. 2011).

1.3.3. The role of MCTs in cancer

High levels of MCTs expression have been associated with carcinogenesis given the increase of lactate production due to Warburg effect (Pinheiro, Longatto-Filho et al. 2008; Pinheiro, Albergaria et al. 2010). The efflux and influx of lactate is mainly mediated by MCT4 and MCT1 isoforms, respectively (Semenza 2008). The presence of MCT4 in the plasma membrane of cancer cells plays a dual function allowing the efflux of intracellular lactate and pH regulation since the efflux of lactate is coupled to the output of a proton, important to prevent intracellular acidification and consequently apoptosis (Figure 6) (Pinheiro, Longatto-Filho et al. 2012). The maintenance of an appropriate intracellular pH is also ensured by others pH regulatory systems in the plasma membrane, such as Na^+/H^+ exchanger (NHE) family, carbonic anhydrase 9 (CA9) and anion exchanger 1 (AE1) (Chiche, Brahimi-Horn et al. 2010).

MCT isoforms are differently upregulated in tumors including colon cancinoma, lung cancer, high grade gliomas, breast cancer, prostate cancer and gastric adenocarcinomas (Pinheiro, Longatto-Filho et al. 2012). MCT1 is upregulated in breast cancer (Pinheiro, Albergaria et al. 2010), colorectal (Pinheiro, Longatto-Filho et al. 2008) and cervical cancer (Pinheiro, Longatto-Filho et al. 2008) associated to poor prognosis. MCT4 is upregulated in cervical (Pinheiro, Longatto-Filho et al. 2008), colorectal (Pinheiro, Longatto-Filho et al. 2008) and prostate cancer (Pertega-Gomes, Vizcaino et al. 2011) and downregulated in gastric cancer (Pinheiro, Longatto-Filho et al. 2009). In a particular aggressive subtype of breast cancer (basal-

like) were observed high expression of MCT1 in the cytosol and in the plasma membrane compared to normal breast epithelium (Pinheiro, Albergaria et al. 2010; Pinheiro, Reis et al. 2010). Moreover, the expression of MCT2 was only present in the cytoplasm at similar levels to normal tissue (Pinheiro, Reis et al. 2010) and MCT4 showed a significant increase in cytoplasm expression compared to normal epithelium (Pinheiro, Albergaria et al. 2010) with no differences in plasma membrane expression. In fact, this study concluded that the high expression of MCT1 alone or in co-expression with CD147 is associated with tumor aggressiveness in breast cancer (Pinheiro, Albergaria et al. 2010).

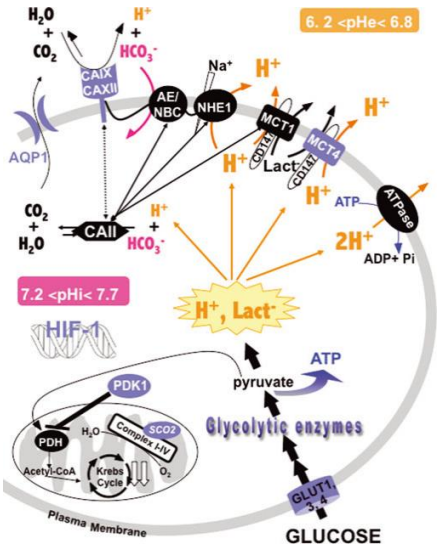

Figure 6. Role of MCTs in cancer cells metabolism (Chiche, Brahimi-Horn et al. 2010).

1.4. Metabolic targeting strategies for cancer therapy

Since metabolic phenotype of cancer cells is the basis for several mechanisms of tumor resistance to traditional therapy it had been explored several anticancer strategies targeting tumor metabolism. Metabolic strategies include indirect targets that consist in signaling pathways that regulates cellular metabolism altered in cancer, and direct targets such as metabolic enzymes (Tennant, Duran et al. 2010) (Figure 7).

The first antimetabolites were designed to inhibiting DNA synthesis. These drugs include 5-fluorouracil (5-FU) and cytarabine (Ara-C) that target the final stages of nucleotide synthesis

pathway, leading to incomplete DNA synthesis and cell death unspecific to cancer cells (Ewald, Sampath et al. 2008).

The aberrant glycolytic phenotype of cancer cells has been explored as a target for direct inhibitors with agents targeting key enzymes of this metabolic pathway (Pelicano, Martin et al. 2006; Tennant, Duran et al. 2010). Glucose transporter 1 (GLUT1) overexpressed in cancer cells, is a target for the agent phloretin (Cao, Fang et al. 2007) with promise results in cell growth inhibition *in vitro* (Devi and Das 1993) and *in vivo* (Nelson and Falk 1993). The first glycolytic enzyme, hexokinase, can be inhibited by both lonidamine and a glucose analog 2-deoxyglucose, currently in clinical trials in combination with others chemotherapeutic agents (Tennant, Duran et al. 2010). Another glycolytic inhibitor is Imatinib or Gleevec that limits hexokinase and glucose-6-phosphate dehydrogenase (G6PD) activity in leukemia cells (Boren, Cascante et al. 2001; Gottschalk, Anderson et al. 2004). The final enzyme of glycolytic pathway is pyruvate kinase (PK) which converts phosphoenolpyruvate (PEP) into pyruvate and an inhibitor of PK, termed TLN-232 has been used in Phase II clinical trials (Tennant, Duran et al. 2010). In lactate fermentation, pyruvate is reduced to lactate by lactate dehydrogenase (LDHA) and pyruvate dehydrogenase kinase 1 (PDHK1) regulates the activity of pyruvate dehydrogenase (PDH) complex. PDHK1 is inhibited by dichloroacetate (DCA) which increased PDH activity and promote switch from glycolysis to OXPHOS reacting mitochondrial function and generation of free radicals which were toxic to tumor growth. Although DCA is not a specific inhibitor for cancer cells (Stockwin, Yu et al. 2010) it induces a decrease in tumor proliferation (Bonnet, Archer et al. 2007).

Several small molecules are known to inhibit the function of MCTs important to support glycolytic metabolism by exporting lactate. MCTs inhibitors can be group into three categories: (i) bulky or aromatic monocarboxylates that act as competitive inhibitors, such as phenyl-pyruvate α-cyano-4-hydroxycinnamate (CHC) (Halestrap 1976); (ii) amphiphilic compounds as flavoniods (quercetin and phloretin) and anion exchanger (AE) inhibitors, such as 5-nitro-2-(3-phenyl-propylamino)-benzoate (NPPB) (Halestrap and Meredith 2004); (iii) stilbene disulphonates as 4,4'-diisothiocyanostilbene-2,2'-disulphonate (DIDS) (Poole and Halestrap 1991). These inhibitors are not specific for one MCT isoform, for instance CHC is a potent inhibitor of MCT1 but can also inhibit MCT2 (Halestrap and Price 1999). Recently, AstraZeneca developed a specific and high affinity inhibitor for MCT1 (AR-C155858) that is a potent immunosuppressive drug inhibiting T lymphocyte proliferation and were subsequently shown to bind to MCT1 and MCT2, but not MCT4 in *in vitro* and *in vivo* (Murray, Hutchinson et al. 2005). The inhibition of MCT1 occurs by

binding to intracellular site involving transmembrane helices 7-10 (Ovens, Davies et al. 2010) and MCT2 inhibition is modulated by association to ancillary protein (Ovens, Manoharan et al. 2010).

MCTs have been also explored as potential gateways to drug delivery particularly drugs with a carboxyl group in their chemical structure (Halestrap and Price 1999; Enerson and Drewes 2003). 3-bromopyruvate (3-BP) has been further explored due to it potential as a metabolic inhibitor that inhibits energy production in form of ATP at both glycolysis and oxidative phosphorylation levels. Animal models showed that 3-BP has been efficient in eradication of tumors of advanced liver cancers *in vivo* when the compound was delivery by local infusion and intravenously, without apparent cytotoxicity effects to normal cells (Geschwind, Ko et al. 2002; Ko, Smith et al. 2004). Moreover, recently was reported a first human translational study that demonstrate 3-BP efficacy and specificity in eradication of tumor, being in preclinical trials (Pelicano, Martin et al. 2006; Tennant, Duran et al. 2010; Ko, Verhoeven et al. 2012).

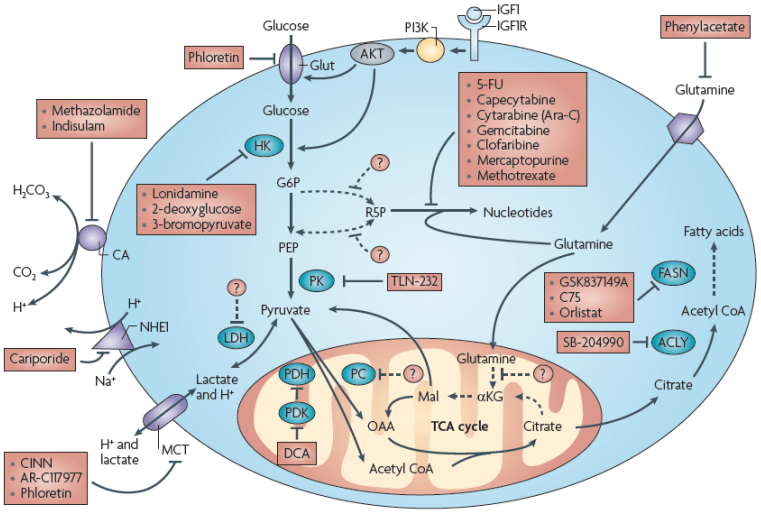

Figure 7. Schematic representation of metabolic targeting tumor strategies (Tennant, Duran et al. 2010). 5-FU – 5-fluorouracil; αKG – α-ketoglutarate; ACLY – ATP citrate lyase; CA – carbonic anhydrase; CINN – α-cyano-4-hydroxycinnamate; DCA – dichloroacetate; FASN – fatty acid synthase; G6P – glucose-6-phosphate; Glut – glucose transporter; HK – hexokinase; IGF1 – insulin-like growth receptor 1; IGF1R – IGF1 receptor; LDH – lactate dehydrogenase; Mal – malate; MCT – monocarboxylate transporter; NHE1 – Na^+/H^+ exchanger 1; OAA – oxaloacetate; PDH – pyruvate dehydrogenase; PDK – pyruvate dehydrogenase kinase; PEP – phosphoenol pyruvate; PK – pyruvate kinase; R5P – ribose 5-phosphate; TCA – tricarboxylic acid cycle

1.4.1. 3-Bromopyruvate as an anticancer agent

3-bromopyruvate (3-BP) is a pyruvate analog with anticancer activity (Ko, Pedersen et al. 2001; Pedersen 2012; Shoshan 2012). This molecule is an alkylating agent able to inhibit the enzymatic function of several proteins by its pyruvylation at a -SH group of cysteine residue (Ko, Verhoeven et al. 2012). 3-BP suppresses both glycolysis and oxidative phosphorylation capacity decreasing the production of intracellular ATP and subsequently cause cell death (Ko, Pedersen et al. 2001).

The most relevant targets of 3-BP to tumor metabolism are the glycolytic enzyme HK II, responsible for the phosphorylation of glucose to glucose-6-phosphate, and the mitochondrial ATP synthasome located in the inner mitochondrial membrane responsible for the generation of ATP (Ko, Pedersen et al. 2001; Ko, Smith et al. 2004; Chen, Zhang et al. 2009; Mathupala, Ko et al. 2009) (Figure 8). 3-BP covalently modify modifies the HKII, leading to its dissociation from the mitochondria and the release of apoptosis-inducing factor (AIF) and cell death (Chen, Zhang et al. 2009).

Several studies have shown that 3-BP also inhibits others glycolytic enzymes such as glyceraldehyde-3-phosphate dehydrogenase (GAPDH) (Ganapathy-Kanniappan, Geschwind et al. 2009; Ganapathy-Kanniappan, Vali et al. 2010), 3-phosphoglycerate kinase (PGK) (Pereira da Silva, El-Bacha et al. 2009), pyruvate kinase (PK) (Acan and Ozer 2001) and non-glycolytic enzymes such as vacuolar-type H^+-ATPase (V-ATPase) (Dell'Antone 2006), 4-aminobutyrate aminotransferase (Blessinger and Tunnicliff 1992), sarco/endoplasmic reticulum calcium Ca^{2+}-ATPase (SERCA) type 1 (Jardim-Messeder, Camacho-Pereira et al. 2012), histone deacetylases (HDAC1 and HDAC3) (Thangaraju, Karunakaran et al. 2009) and mitochondrial succinate dehydrogenase (Pereira da Silva, El-Bacha et al. 2009). Therefore, the effect of 3-BP include alteration in mitochondria dynamic by mitochondrial depolarization, decrease in cellular ATP levels from glycolysis and mitochondrial respiration (Pedersen 2007; Ihrlund, Hernlund et al. 2008), induction of apoptosis pathway by release of apoptosis-inducing factor (AIF) (Kim, Ahn et al. 2008) and induction of endoplasmatic reticulum stress which inhibits protein synthesis (Ganapathy-Kanniappan, Geschwind et al. 2010) that lead to cell death. Although 3-BP targets have been identified, the precise mechanism of its uptake into cancer cells is poorly understood. Transport studies in *Xenopus laevis* oocytes expressed human SLC5A8 (SMCT1) and ectopic expression of SMCT1 in human breast cancer cell line MCF7 demonstrated that SMCT1 is involved in the transport of 3-BP into cells (Thangaraju, Karunakaran et al. 2009). Moreover, a

recent haploid cell genetic screening study performed in human leukemia cell line KBM7 showed that MCT1 is also involved in the transport of 3-BP (Birsoy, Wang et al. 2013).

Some studies demonstrated that 3-BP eradicate several types of tumors of advanced cancers. 3-BP anticancer effect was reported in human breast cancer by our group and others (Buijs, Vossen et al. 2009; Queiros, Preto et al. 2012), in rabbit VX2 model of hepatocarcinomas (Ko, Smith et al. 2004), in rabbit liver cancer (Ko, Pedersen et al. 2001; Geschwind, Ko et al. 2002; Vossen, Buijs et al. 2008), in lung cancer (Zhang, Pan et al. 2012) and in mesothelioma (Philippe, Xiao-Dong et al. 2012). Moreover, 3-BP in combination with chemotherapeutic drugs induced a dose-dependent effect. 3-BP has a significant combinatory effect with cisplatin and oxaliplatin in HCT116 colon carcinoma cell line (Ihrlund, Hernlund et al. 2008). Combination with rapamycin show highly synergistic effect in both killing leukemia and lymphoma cells (Xu, Pelicano et al. 2005). The action of these two agents promotes the depletion of cellular ATP, and caused dephosphorylation of the mTOR downstream target molecules. In C6 glioma cells, the combination of 3-BP with citrate (inhibitor of phosphofructokinase) deplete ATP and block migratory capacity (El Sayed, El-Magd et al. 2012). More recently, it was also reported a first human patient case with fibrolamellar hepatocellular carcinoma known to treated with 3-BP, that demonstrate the eradication of tumor without apparent cytotoxicity to normal cells (Ko, Verhoeven et al. 2012). Several *in vitro* and *in vivo* studies with 3-BP demonstrates its potential clinical use as an anticancer agent.

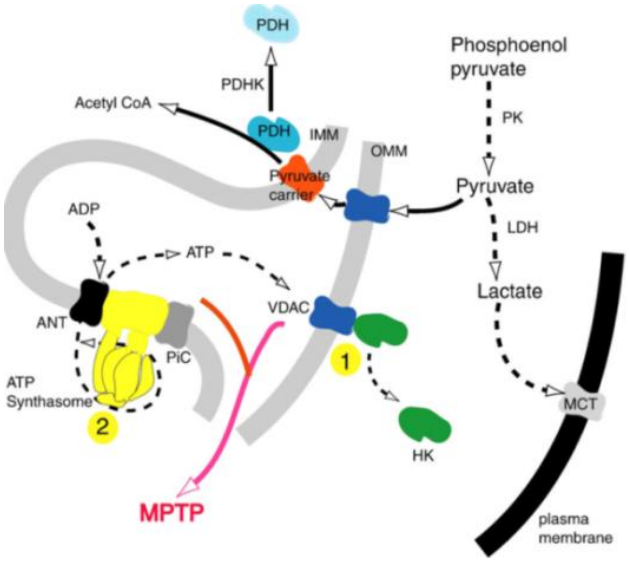

Figure 8. Main targets of 3-bromopyruvate molecule in cancer cells: (1) hexokinase II and (2) ATP synthasome (Mathupala, Ko et al. 2009).

1.5. Butyrate anti-carcinogenic potential in cancer cells

Short-chain fatty acids (SCFAs), proprionate, acetate and butyrate are produced by colonic bacterial fermentation of dietary fiber in the intestinal lumen (Hamer, Jonkers et al. 2008). The production of butyrate is important for the maintenance of colonic homeostasis by inducing cell maturation, differentiation and apoptosis pathways (Gupta, Martin et al. 2006). Butyrate is a major primary energy source for colonocytes (Fleming, Fitch et al. 1991). At high levels (2-5 mM) function as a inhibitor of histone deacetylases (HDAC) resulting in hyperacetylation of histones and consequent decrease in their affinity for binding DNA and hence increases the accessibility for transcription genes silenced at epigenetic level (Donohoe, Collins et al. 2012). At low doses (0.5-1 mM) butyrate is metabolized in the mitochondria to acetyl-CoA by β-oxidation followed by TCA cycle to yield citrate. Citrate is exported to the cytosol and converted to acetyl-CoA by the enzyme ATP citrate lyase (ACL). In the nucleus, acetyl-CoA is a cofactor and acetyl-group donor for histone acetyltransferases (HATs) that promotes acetylation of histones (Figure 9) (Donohoe, Collins et al. 2012).

As all weak carboxylic acids, SCFAs are partially ionized in solution. SCFAs have a pKa value approximately of 4.8, and more than 90% exist in the anionic form (dissociated form), ionized in physiologic conditions in the lumen (Hamer, Jonkers et al. 2008). Butyrate can be transported across the colonocyte apical membrane by simple diffusion of the undissociated form that is lipid soluble (Velazquez, Lederer et al. 1997), bicarbonate exchanger SCFA/HCO_3^- (Kawamata, Hayashi et al. 2007) and also by active transport of dissociated form by MCT1 (Cuff, Dyer et al. 2005) and SMCT1 (Gupta, Martin et al. 2006; Thangaraju, Cresci et al. 2008)

The role of butyrate in intestinal lumen has been associated to anti-inflammatory and anti-tumor activity (Inan, Rasoulpour et al. 2000; Hamer, Jonkers et al. 2008). In normal colonocytes low doses of butyrate (0.5-1 mM) promotes cell proliferation by HAT activity, in contrast to its effects on cancerous colonocytes. This opposite effect has been referred as “Butyrate paradox” and is poorly understood. The fact that butyrate at high levels can act as an HDAC inhibitor has been recently linked to this inhibitory growth effect in cancerous colonocytes (Donohoe, Collins et al. 2012). The upregulation of glycolysis in cancerous colonocytes due to the Warburg effect, results in accumulation of butyrate non metabolized in the nucleus where function as HDAC inhibitor to regulate genes that inhibited cell proliferation and promoted apoptosis (Donohoe, Collins et al. 2012).

Recently, our group demonstrated that pre-incubation with butyrate enhanced significantly 3-BP cytotoxicity effect, especially in the most resistant human breast cancer cell line, SK-BR-3. Butyrate induced localization of MCT1 in the plasma membrane, as well as overexpression of MCT4 and its chaperon CD147 which were accompanied by an increased sensitivity to 3-BP cytotoxic effect (Queiros, Preto et al. 2012).

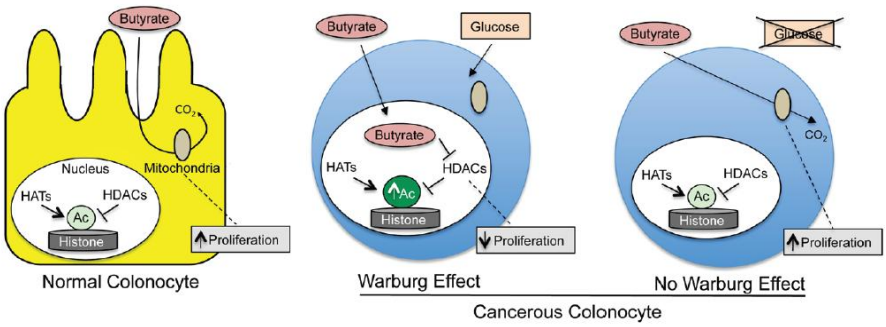

Figure 9. Schematic overview of butyrate dual function in energetics and epigenetics in normal and cancerous colonocytes in the intestinal lumen. Butyrate is a primary energy source for normal colonocyte and is metabolized by β-oxidation to acetyl-CoA which is a cofactor for histone acetyltransferases (HATs) that regulate gene expression in the nucleus. In cancerous colonocyte that exhibit Warburg effect, butyrate accumulates in the nucleus where function as histone deacetylases inhibitor (HDACs) regulating (Donohoe, Curry et al. 2013).

1.6. Breast cancer

Breast cancer is the most diagnosed malignancies and the leading cause of death related to cancer in women (Jemal, Bray et al. 2011). The incidence and mortality of this disease is growing and in 2008, were diagnosed 23% new cases of breast cancer and 14% of deaths related to cancer worldwide (Jemal, Bray et al. 2011). There are several factors that contribute to the risk of development breast cancer, such as environmental, hormonal, lifestyle, and genetic factors. The lifestyle related factors include late age of first pregnancy, oral contraceptive, hormone therapy after menopause, obesity and alcohol (Jemal, Center et al. 2010). Breast cancer family history is also an important risk factor, being *BRCA1* and *BRCA2* genes (breast cancer genes 1 and 2) the most predominant genetic mutations in hereditary breast cancer (King, Marks et al. 2003).

Breast cancer displays a variety of phenotypes at histological and molecular levels. The development of human breast cancer can start in epithelial cells of the mammary tissue, usually in the ductal luminal cells or in the terminal ductal lobular units (TDLUs) (Visvader 2009). According to the gene expression profiles, breast cancer can be cluster in five major molecular subtypes: luminal A (ER^+ and/or PR^+, $HER\text{-}2^-$), luminal B (ER^+ and/or PR^+, $HER\text{-}2^+$), $HER2^+$ (ER^-, PR^-, $HER\text{-}2^+$), basal-like (ER^-, PR^-, $HER\text{-}2^-$) and normal-like (claudin-low) (Sorlie, Perou et al. 2001). The most important characteristic of these subtypes is the expression of progesterone receptor (PgR), estrogen receptor (ER) and human epidermal growth factor receptor-2 (HER-2) (Sotiriou, Neo et al. 2003). The luminal subtype is characterized by the expression of ER; luminal A and B subtypes distinguish from each one by the absence or presence of HER-2 receptor, respectively. The molecular profile of HER-2 subtype shows the expression of HER-2 receptor. The basal-like subtype known as triple-negative breast cancer is distinguished by the absence of ER, PR and HER-2 receptors expression (Hudis and Gianni 2011).

Treatment of breast cancer depends on the subtype of cancer and on its stage of evolution. Actually, there are several strategies that consists in local or systemic treatments (Al-Ejeh, Smart et al. 2011). Local treatments include surgery and radiotherapy, and systemic treatments comprise chemotherapy, hormonal therapy or target therapy. Multidrug resistance and limitations in breast cancer chemotherapy emphasizes the need for new drugs to increase treatment efficacy (Li, Lewis et al. 2008). The mechanistic understanding of the molecular and biochemical events that occur in cancer cells is the starting point for the development of new treatments for breast cancer.

2. Rationale and Aims

Rationale

3-Bromopyruvate (3-BP) is an alkylating agent that acts in glycolytic metabolism inhibiting the activity of enzymes, such as hexokinase II which is overexpressed in cancer cells (Ko, Pedersen et al. 2001). This molecule has been further explored due to it potential as anticancer agent in the eradication of tumors *in vitro* and *in vivo* without cytotoxicity to normal cells (Ko, Pedersen et al. 2001; Ko, Smith et al. 2004). Monocarboxylate transporters (MCTs) are responsible for the transport of endogenous monocarboxylic acids such as pyruvate, lactate and butyrate (Halestrap and Wilson 2012) and exogenous monocarboxylates as 3-BP (Birsoy, Wang et al. 2013) across the plasma membrane. Little was known about the role of butyrate in the effect of 3-BP in cancer cells. Previous observations in our laboratory showed that pre-incubation with butyrate sensitized cells to 3-BP cytotoxic effect in the most resistant human breast cancer cell line, SK-BR-3 (Queiros, Preto et al. 2012). These observations also indicated that butyrate promoted the localization of MCT1 at the plasma membrane and enhanced the expression of MCT4 and its chaperon CD147 (Queiros, Preto et al. 2012). Knowing that butyrate can alter the expression of MCTs, the hypothesis that butyrate could regulate the cytotoxic effect of 3-BP was explored in this work.

Aims

This work aimed to characterize the effect of butyrate without or with 3-BP in four human breast cancer cell lines with different sensibilities to 3-BP (ZR-75-1> MCF-7> MDA-MB-231> SK-BR-3), and evaluate the expression of MCTs in these conditions. Our specific aims were the:

1. Characterization of basal expression profile of MCTs and ancillary proteins important for their function, through western blot assay;
2. Evaluation of cytotoxic effect of butyrate without or with 3-BP, by trypan blue exclusion assay;
3. Evaluation of MCTs expression upon treatments, through western blot assay;
4. Optimization of MCT1 and MCT4 silencing by RNA interference (RNAi) to further study its role in 3-BP effect;
5. Evaluation the effect of butyrate without or with 3-BP on cell cycle by flow cytometry.

3. Materials and Methods

3.1. Cell lines and culture conditions

In this study human breast cancer cell lines ZR-75-1, MCF-7, MDA-MB-231 and SK-BR-3 were used. ZR-75-1 cell line is derived from ductal adenocarcinoma of mammary gland, subtype luminal A and is estrogen receptor positive (ER^+). MCF-7 is derived from mammary gland adenocarcinoma, subtype luminal A, ER^+. MDA-MB-231 is derived from adenocarcinoma of mammary gland, subtype basal and is ER^-. SK-BR-3 is derived from mammary gland adenocarcinoma, subtype $HER2^+$ and is ER^-. All cell lines were obtained from American Type Culture Collection (ATCC, EUA).

Cells were cultured in RPMI-1640 medium (PAA) supplemented with 10% heat inactivated fetal bovine serum (FBS) (Gibco, Life Technologies) and 1% antibiotic solution (penicillin-streptomycin solution) (Gibco, Life Technologies), incubated at 37ºC under a humidified atmosphere with 5% CO_2, in an incubator. For the cell line MCF-7 the growth medium was also supplemented with 25 μg/ml insulin (Sigma). The maintenance of cell culture in 25 cm^2 polystyrene culture flasks (T25 flasks) (TPP), in exponential growth phase, was achieved by subculture when 80% confluence was reached, by treatment with 0.05% trypsin/EDTA solution (Sigma).

3.2. Preparation of carboxylic acid solutions

Butyric acid and 3-bromopyruvate (3-BP) were purchased from Sigma and their solutions prepared in phosphate-buffered saline (PBS) at the concentrations of 200 mM and 12 mM, respectively, and further diluted in PBS to the desired final concentrations. Butyric acid solutions were adjusted to pH 7.4 and stored at 4ºC in the maximum period of one week, and 3-BP solutions were prepared freshly at the days of treatment. All the solutions were sterilized by filtration (0.22 μm syringe filter units) before use and their addition to the culture medium never exceeded 10% of the final volume.

3.3. Treatment conditions

For treatment with butyric acid and 3-BP, cells in exponential growth phase were cultured in 6-well plates at a cellular density defined for each cell line and incubated at 37ºC in a 5% CO_2 atmosphere during 24 hours, to allow cell adhesion. ZR-75-1, MCF-7 and SK-BR-3 were plated at a density of 250 000 cells per well and MDA-MB-231 was plated at 200 000 cells per well (final volume 1.5 ml/well). After 24 hours, culture medium was removed and replaced by fresh media containing different concentrations of butyric acid (0.5 mM and 10 mM) alone or in combination with the 3-BP in a concentration corresponding to the respective IC_{50} (half maximal inhibitory concentration) for each cell line (Table II). After treatment, cells were incubated for a further 16 hours at 37ºC, 5% CO_2. For the negative controls fresh medium without butyric acid or 3-BP was added.

Table II. IC_{50} values of 3-bromopyruvate for the breast cancer cell lines ZR-75-1, MCF-7, MDA-MB-231 and SK-BR-3 used in this study (Queiros, Preto et al. 2012; Pacheco 2012). 3-BP – 3-bromopyruvate

Cell line	3-BP IC_{50} (μM)
ZR-75-1	55.7 ± 1.5
MCF-7	84.6 ± 15.4
MDA-MB-231	148.6 ± 28.1
SK-BR-3	458.1 ± 28.6

3.4. Trypan Blue exclusion assay

Trypan Blue exclusion assay is a quick and reproductive method to evaluate cell viability. This is an impermeable dye that cannot penetrate the membrane of viable cells but can permeate non-viable cells, due to their compromised membrane resulting in a blue coloration.

After applying the treatments described above, adherent cells were gently washed with PBS and trypsinized with 0.05% trypsin/EDTA at 37ºC. The culture medium and the cell suspension were collected together in a centrifuge tube and then a sample of this suspension was mixed with 0.4% trypan blue solution (1:2, cell suspension:trypan blue). After a 5 minutes incubation at room temperature, viable cells (clear cells) and non-viable cells (blue staining cells)

were counted in a hemacytometer under a bright-field microscope. The viability was determined by dividing the number of viable cells by the total number of cells, and expressed as a percentage.

3.5. Protein extraction and Western Blot analysis

3.5.1. Total protein extraction

For the expression analysis of proteins at basal condition, cells were plated in 6-well plates (final volume 1.5 ml/well) at a density of 500 000 cells for ZR-75-1 and SK-BR-3, 350 000 cells for MCF–7 and 300 000 cells for MDA-MB-231 per well, for 24 hours. For the expression analysis of proteins after carboxylic acids treatment, ZR-75-1, MCF-7 and SK-BR-3 were plated at a density of 250 000 cells per well and MDA-MB-231 was plated at 200 000 cells per well in a 6-well plates (final volume 1.5 ml/well) for 24 hours. Cells were treated with different concentrations of butyric acid (0.5 mM and 10 mM) alone or in combination with respective 3-BP IC_{50} for each cell line, for 16 hours. After appropriate treatment, culture medium containing floating cells was recovered to a centrifuge tube and maintained on ice. Adherent cells were washed with PBS, trypsinized and collected to the same centrifuge tube. Cells were centrifuged at 2000 rpm for 10 minutes at 4°C and pellets (500 µl) were transferred to eppendorfs tubes and 500 µl PBS were added. Pellets were centrifuged at 2000 rpm for 5 minutes at 4°C and supernatant was discarded. Then, 30 µl of ice-cold lysis buffer (150 mM NaCl, 0.1 mM EDTA, 1% Triton X-100, 1% NP40, 50 mM Tris-HCl pH 7.5) supplemented with 1/7 protease inhibitor cocktail (Roche Applied Sciences), was added to each sample and resuspended. Samples were incubated on ice during 10 minutes, occasionally vortexed. Cell lysates were centrifuged at 13 000 rpm for 15 minutes at 4°C. Supernatants were collected to a new eppendorf tube and stored at -80°C until western blot assay.

3.5.2. Protein Quantification

Protein concentration was determined by BCA Protein Assay kit (Thermo scientific) which is a colorimetric assay based on Cu^{+2} reduction to Cu^{+1} by protein in an alkaline medium (biuret

reaction). The purple-colored reaction product exhibits a high absorbance at 562 nm directly proportional to protein concentration.

Diluted bovine serum albumin (BSA) standards and working reagent (50:1, Reagent A:B) were prepared according to the standard protocol. In a 96-well plate 200 µl of working reagent were added to 10 µl of BSA standards or samples of total protein extracts diluted 1:20 in proper buffer. After incubation at 37ºC for 30 minutes, absorbance was measure at 562 nm in a microplate reader (Spectra Max 340-PC, Molecular Devices). The protein concentrations of total protein extracts were obtained using the standard curve with the absorbance of BSA standards versus its concentration in µg/ml, and considering the dilution factor of the sample.

3.5.3. Western Blot assay

After total protein extraction and protein quantification described above, samples were processed to Western Blot assay. For that purpose, 25 µg of total protein samples were mixed with 5 µl of Laemmli Sample Buffer (final volume 25 µl) and denatured at 95ºC for 5 minutes, followed by a shot spin. After protein denaturation, samples were separated electrophoretically on 10% polyacrylamide gel (resolving gel solution: 375 mM Tris-HCl pH 8.8 SDS 0.4%, 15% glycerol, 0.1% TEMED, 0.05% APS; stacking gel solution: 125 mM Tris-HCl pH 6.8 SDS 0.4%, 0.1% TEMED, 0.05% APS). Molecular weight marker (Precision Plus Protein™ Dual Xtra Standards, BioRad) was used in all the blots to access protein size. The electrophoresis was performed in a Mini Protean Tetra System (Bio-Rad) electrophoresis system at 10 mA for 2 hours, using running buffer (0.025 M Tris base, 0.192 M Glycine, 0.1% SDS).

The proteins separated in the polyacrylamide gel were then transferred to a polyvinylidene difluoride (PVDF) membrane (Millipore) previously hydrated with methanol. Electrotransfer occurred in a Mini Protean Tetra System (BioRad) at 54 mA for 1 hour, using transfer buffer (0.025 M Tris base, 0.192 M Glycine, 0.1% SDS, 20% methanol). Membranes were rinsing with PBS and blocked in PBS-T (PBS with 0.1% Tween-20) containing 5% non-fat dry milk (Molico) for 1 hour at room temperature or overnight at 4ºC, to block non-specific biding sites. Then, membranes were washed with PBS-T and incubated with the specific primary antibodies diluted in PBS-T with 5% non-fat dry milk or 5% BSA, overnight at 4ºC, with agitation in a Roller Mix. After overnight, membranes were washed three times for 5 minutes with PBS-T to remove excess of

unbound antibody followed by incubation with appropriate secondary antibodies conjugated with IgG horseradish peroxidase diluted in PBS-T during 1 hour at room tempetature, with agitation in a Roller Mix. Membranes were washed three times with PBS-T for 15 minutes and protein immunodetection was revealed by chemiluminescence detection kit (Millipore), using the Chemi Doc XRS (BioRad). The intensity of bands was quantified using the ImageJ software and β-actin was used as internal control. The results of tree independent experiments were quantified and correspondent values were divided by the β-actin value. In order to reprobe with other antibodies, membranes were stripped with stripping glycine buffer (7.5 g Glycine, 0.5 g SDS, 5 ml Tween-20, pH 2.2) for two times during 10 minutes at room temperature following by two times washes for 10 minutes with PBS-T. All primary antibodies and secondary antibodies and their dilutions used in this study are listed in Table III.

Table III. List of primary and secondary antibodies conditions used in this study. FG – fully glycosylated; CG – core glycosylated.

Protein	Size (kDa)	Primary antibody (company (reference); dilution)	Secondary antibody (Jackson laboratories; dilution 1:5000)
MCT1	43	Santa Cruz (sc-365501); 1:500 (5% milk)	Anti-mouse
MCT2	35	Santa Cruz (sc-14926); 1:500 (5% milk)	Anti-mouse
MCT4	43	Santa Cruz (sc-50329); 1:500 (5% BSA)	Anti-rabbit
AE1 (Band 3)	50	Abcam (ab-108414); 1:500 (5% milk)	Anti-rabbit
CD147	45-65 (FG) 35 (CG)	Santa Cruz (sc-71038); 1:100 (5% milk)	Anti-mouse
CD44	83	Serotec (MCA2726); 1:500 (5% milk)	Anti-mouse
β-actin	30	Santa Cruz (sc-47778); 1:2000 (5% BSA)	Anti-mouse

3.6. Cell cycle analysis

Flow cytometry allows a quantitative characterization of multiple parameters of individual cells and their populations. Cell cycle analysis performed by flow cytometry allows a precise measurement of cellular DNA content and assessing the percentage of cells in the individual cell-cycle phases of interphase determined by peaks in a DNA content frequency histograms (Côrte-Real, Sansonetty et al 2002).

After appropriate treatments with carboxylic acids, medium containing floating cells and adherent cells trypsinized were collected to the same centrifuge tube, and centrifuged at 500 g for 3 minutes. The pellet was ressuspended in 500 μl and incubated on ice for 15 minutes. After this period, 1.5 ml of 100% cold ethanol (stored at -20ºC) was added to pellet and incubated on ice during 15 minutes, to allow cell fixation. Cells were then washed with 3 ml PBS, centrifuged at 500 g for 3 minutes at 4ºC and the pellet was washed with PBS. The final pellet was ressuspended in 500 μl PBS and incubated with 50 μl of RNase A solution (200 μg/ml in sodium citrate (1% w/v)) at 37ºC for 15 minutes, to eliminate RNA. After 15 minutes incubation, 50 μl propidium iodide (PI) staining solution (0.5 mg/ml in sodium citrate (1% w/v)) was added and after vortex cells were incubated at room temperature for 30 minutes in the dark. Cells with red fluorescence (FL-3 channel (488/620 nm)) were analyzed in Epics XL flow cytometer (Beckman Coulter) with an average of 20 000 counts per sample. Data were analyzed with the FlowJo software to generate DNA content frequency histograms and quantify the amount of cells in each phases of interfase, including sub-G1 population assumed as death cells (cells with less than normal amount of DNA content).

3.7. Fluorescence microscopy: actin evaluation

ZR-75-1 and SK-BR-3 cells were cultured in 24 well-plates at a cell density of 150 000 cells per well (final volume 500μl/well) and incubated at 37ºC with 5% CO_2 during 24 hours to adhere. Then, cells were treated with 3-BP in a concentration corresponding to the respective IC_{50} for each cell line, as described above, and in controls medium was refreshed. After 16 hours of proper incubation, medium with floating cells was discarded and adherent cells were washed with prewarmed PBS (pH 7.4) two times, and fixed with 3.7% formaldehyde solution in PBS for 10 minutes at room temperature. After fixation, cells were washed twice with PBS. Then permeabilized with 0.1% Triton X-100 in PBS for 4 minutes, washed with PBS and incubated with Alexa Fluor 488 Phalloidin (Gibco, Life Technologies) fluorescent probe with high affinity to filamentous actin (F-actin) diluted 1:40 in PBS for 20 minutes at room temperature, protecting from light. For double staining, cells were subsequently incubated with Vectashield Mounting Medium with DAPI (Vector Laboratories) for 20 minutes, to stain nucleus. Cells were washed twice with PBS to remove the excess labeling and photographed using fluorescence microscope Olympus IX71.

3.8. Silencing of MCTs by RNA interference assay

RNA interference (RNAi) is a mechanism for silencing gene expression by targeting a specific mRNA to degradation. Small interfering RNA (siRNA) is the main effector of the post-transcriptional gene silencing. In the cell, the siRNA is recognized and incorporated by RNA-induced silencing complex (RISC) that leads to the cleavage of sense strand of RNA by argonaute 2 (AGO2). Subsequently, the active complex RISC-siRNA binds and degrades complementary mRNA resulting in the silencing of specific target gene (Agrawal, Dasaradhi et al. 2003).

The inhibition of MCT1 and MCT4 expression in the different breast cancer cell lines was performed by RNAi. For the optimization of RNAi transfection conditions according to reverse transfection method a fluorescent control siRNA non-target labeled with Alexa Fluor 488 (all stars negative siRNA, AF-488, Qiagen) was used and the efficacy and cytotoxicity of transfection reagent Lipofectamine RNAiMAX (Invitrogen) in delivery exogenous siRNA to cells were assessed by fluorescence microscopy and trypan blue exclusion assay, respectively.

3.8.1. Optimization of RNAi transfection conditions

The optimization of siRNA transfection conditions in ZR-75-1, SK-BR-3 and MCF-7 cell lines were performed according to reverse transfection method (Gallagher, Castorino et al. 2007).

For the transfection mix, 0.5, 1 and 2 µl of transfection reagent Lipofectamine RNAiMAX (Invitrogen) were diluted in Opti-MEM (Reduced serum medium) (Gibco) and incubated 5 minutes at room temperature. After incubation, 5 nM of fluorescent control siRNA non-target labeled with Alexa Fluor 488 (all stars negative siRNA, AF-488, Qiagen) were added to a transfection mix (final volume of 250 µl) and incubated more 15 minutes at room temperature. Controls were performed with Opti-MEM alone. Cells were plated in 6-well plates at a density of 100 000 cells for ZR-75-1 and MCF-7, and 50 000 cells for SK-BR-3 per well (final volume 1.5 ml/well). Cell suspension was prepared in RPMI supplemented with 10% heat inactivated FBS without penicillin/streptomycin antibiotic. Transfection mix and 750 µl of cell suspension previously prepared were distributed by each condition in 6-well plates with coverslips and incubated at 37ºC with 5% CO_2 for 24 hours, to cells adhere. All transfections were performed with solutions

and materials RNAse free. After 24 hours, medium was refreshed with RPMI complete medium supplemented with 10% heat inactivated FBS and 1% penicillin/streptomycin.

In the fourth day of silencing, the cellular uptake of fluorescent control siRNA non-target labeled with Alexa Fluor (siRNA-AF) was accessed by fluorescence microscopy and the cytotoxicity of transfection was determined by trypan blue exclusion assay. For the fluorescence microscopy, cells grown in coverslips were washed with PBS and fixed with 4% paraformaldehyde (PFA) during 30 minutes at room temperature. After fixation, coverslips were mounted in Vectashield Mounting Medium with DAPI (Vector Laboratories) to stain nucleus and photographed by Leica DM 500B fluorescence microscope in appropriate protocol in LAS AF software (Leica). Cells with green fluorescence in the cytoplasm were considered to contain internalization of siRNA-AF. Cytotoxic evaluation of the transfection reagent Lipofectamine RNAiMAX was performed by trypan blue exclusion assay as described above. The viability was determined by dividing the number of viable cells by the total number of cells and expressed as a percentage.

3.8.2. MCT1 and MCT4 silencing by RNAi

MCT1 and MCT4 expression was silenced with siRNA using transfection conditions optimized for reverse method. siRNAs were purchased from Ambion. ZR-75-1 and SK-BR-3 cells were transfected with siRNAs specific for MCT1 (SLC16A1 siRNA, catalog number 4390824) and MCT4 (SLC16A3 siRNA, catalog number 4390824) using Lipofectamine RNAiMAX (Invitrogen). The non-silencing siRNA control (catalog number 4390843) was used as negative control. siRNA transfection was performed using and 1 μl, 2 μl of Lipofectamine RNAiMAX for ZR-75-1 and SK-BR-3, respectively, and 5 nM, 10 nM of siRNA. Knockdown of target genes were confirmed at the protein level by western blot analysis in the fourth and/or fifth day of silencing.

3.9. Statistical analysis

The results are represented as mean ± standard error of the mean (SEM) of at least three independent experiments. Statistical analyses were performed using GraphPad Prism Software v5.00 (California, USA). A p value < 0.05 was considered statistically significant.

4. Results

4.1. Basal expression profile of MCTs and ancillary proteins in breast cancer cell lines

The expression of MCT1, MCT4, CD147, CD44 and AE1 was evaluated by western blot assay in ZR-75-1, MCF-7, MDA-MB-231 and SK-BR-3 human breast cancer cell lines using specific antibodies. Our results showed that the four breast cancer cell lines presented different expression profile for the analyzed proteins (Figure 10).

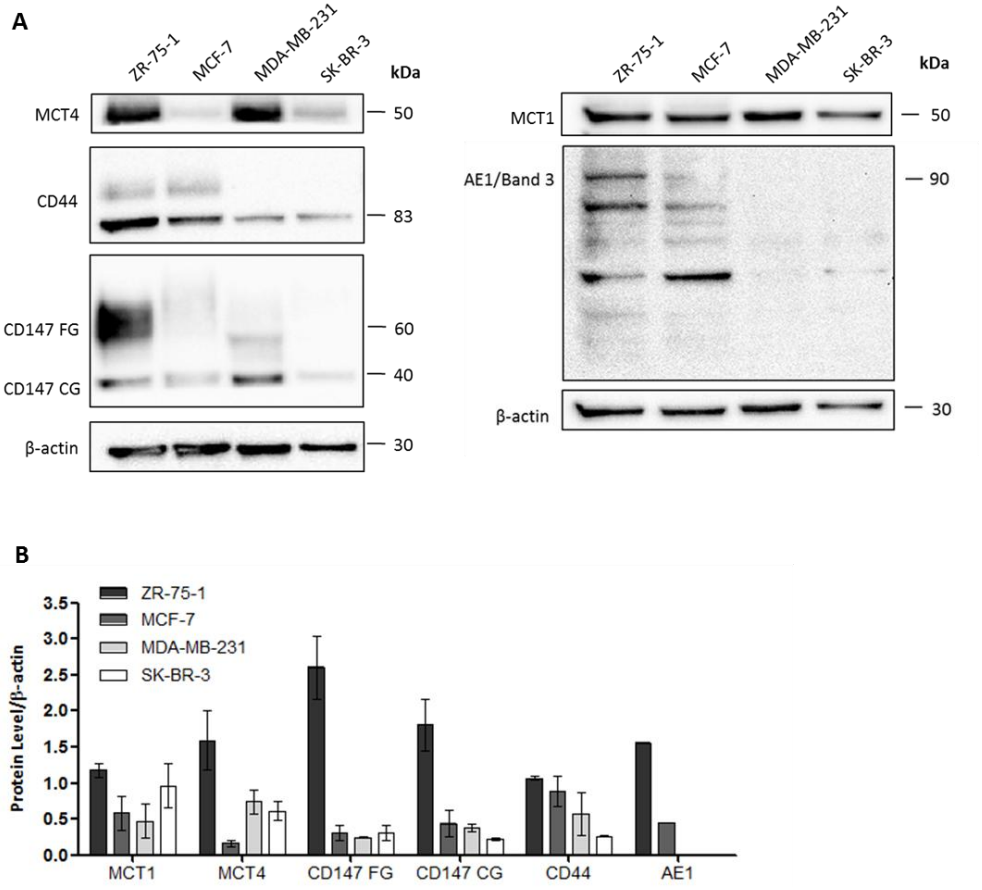

Figure 10. Expression analysis of MCT1, MCT4, CD147, CD44 and AE1 in ZR-75-1, MCF-7, MDA-MB-231 and SK-BR-3 breast cancer cell lines at basal conditions. (A) Western blot of all proteins tested as indicated in the left part of the blots. Protein molecular weights observed are consistent to describe for these proteins and are showed at the right of the blots. β-actin level was used as loading control. A representative experiment of at least three independent experiments is shown. (B) Quantification of proteins levels. Bands were quantified in ImageJ software and values are expressed as mean ± standard error of the mean (SEM) of at least three independent experiments. FG – Fully glycosylated; CG – core glycosylated

MCT1 protein expression was detected in all cell lines, while MCT4 was highly expressed in ZR-75-1 and MDA-MB-231 and at low levels in MCF-7 and SK-BR-3. CD147, a ancillary protein, was expressed in all cell lines, although with different expression levels. The maturated form of CD147 fully glycosylated (FG) (45-65 KDa) and immature form core glycosylated (CG) (35-40 KDa) were highly expressed in ZR-75-1 and at very lower levels in SK-BR-3. CD44, a ancillary protein, was expressed in all cell lines, however, MDA-MB-231 and SK-BR-3 expressed this protein at very low levels. AE1/Band 3, a pH regulator system, showed multiple bands being the band of 90 kDa the membrane protein that was only expressed in ZR-75-1 and MCF-7, presenting higher levels in ZR-75-1 cell line.

4.2. Effect of butyrate and 3-BP treatment on cell viability

The effect of butyrate, applied without or with 3-BP IC_{50}, on cell viability of breast cancer cell lines was evaluated by the Trypan Blue exclusion assay. Cells were treated with two concentrations of butyrate (0.5 mM and 10 mM) alone or in combination with the respective 3-BP IC_{50} for each cell line, for 16 hours. The Trypan Blue exclusion assay results showed different effects on cell viability in response to treatment with butyrate alone or butyrate in co-incubation with 3-BP IC_{50} (Figure 11).

Butyrate decreased the percentage of viable cells dependent on its concentration in all cell lines. In ZR-75-1 and MCF-7, the cell lines more sensitive to 3-BP, treatment with 0.5 mM butyrate resulted in cell viability similar to negative control, being 101% for ZR-75-1 and 99% for MCF-7. Treatment with 10 mM butyrate decreased the percentage of viable cell to 63% in ZR-75 cells and to 79% ($p<0.05$) in MCF-7 cells compared to the negative control. However, co-incubation of 0.5 mM butyrate with 3-BP IC_{50} resulted in cell viability similar to treatment with 3-BP IC_{50} alone being approximately 45% in both ZR-75-1 and MCF-7 cell lines, while the co-incubation of 10 mM butyrate with 3-BP IC_{50} resulted in increased percentage of viable cell being 90% ($p<0.05$) and 87% ($p<0.001$) in ZR-75-1 and MCF-7, respectively compared to treatment with 3-BP IC_{50} alone. In MDA-MB-231 cells, treatment with 0.5 mM butyrate did not altered the percentage of viable cells being 99%, while treatment with 10 mM butyrate decreased cell viability to 71% ($p<0.05$) compared to negative control. Co-incubation of 0.5 mM butyrate with 3-BP IC_{50} increased the percentage of viable cells being 78%, while co-incubation of 10 mM

butyrate with 3-BP IC_{50} has no effect on the percentage being 58%, compared to treatment with 3-BP IC_{50} alone. In SK-BR-3 cell line, the cell line more resistant to 3-BP, treatment with 0.5 mM butyrate reduced the percentage of cell viability to 85% ($p<0.05$), while treatment with 10 mM butyrate decreased to 77% ($p<0.001$) compared to negative control. Co-incubation of 0.5 mM butyrate with 3-BP IC_{50} increased the percentage of cell viability to 90% ($p<0.001$) compared to treatment with 3-BP IC_{50} alone, while treatment of 10 mM butyrate with 3-BP IC_{50} increased the percentage of viable cells to 82% ($p<0.05$) compared to treatment with 3-BP IC_{50} alone. Observation of cells under the microscope showed cellular confluence at 16 hours after treatment with butyrate (0.5 and 10 mM) alone or in combination with 3-BP IC_{50} for each breast cancer cell line (Figure 12), confirming the results of Trypan Blue exclusion assay (Figure 11).

Simultaneous treatment of 0.5 mM butyrate with 3-BP IC_{50} potentiated the effect of 3-BP in the cell lines more sensitive to 3-BP, ZR-75-1 and MCF-7, but not in the most resistant cell lines MDA-MB-231 and SK-BR-3.

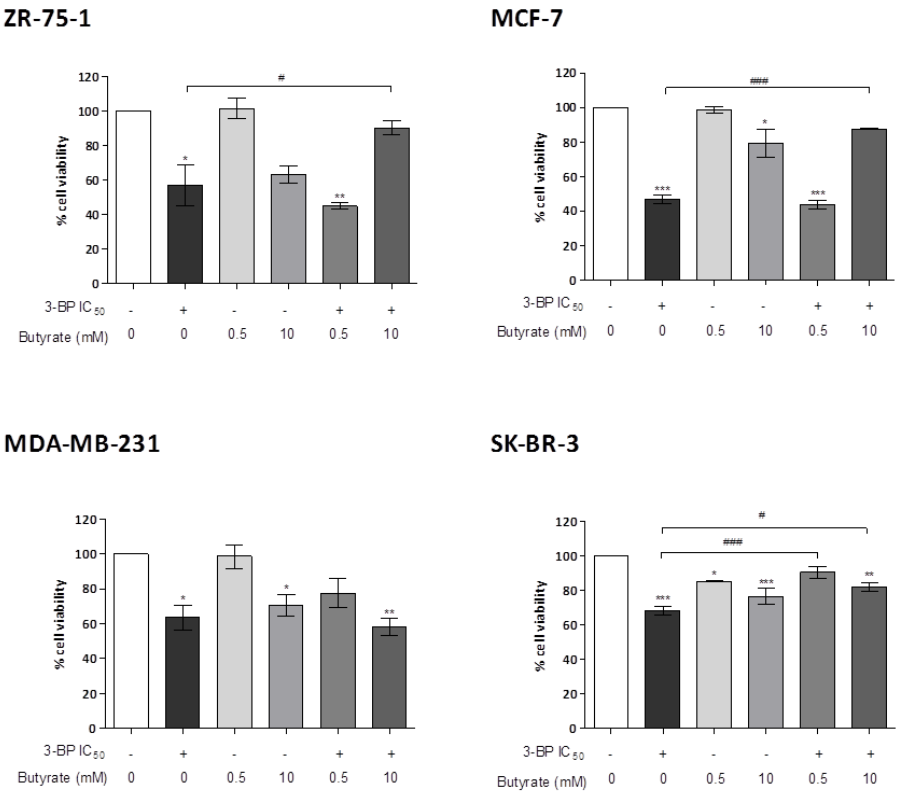

Figure 11. Effect of butyrate (0.5 mM and 10 mM) alone or in combination with 3-BP IC_{50} on cell viability of ZR-75-1, MCF-7, MDA-MB-231 and SK-BR-3 breast cancer cell lines, after 16 hours of incubation. At 16 hours after treatment, cells were collected, stained with trypan blue and counted. Cells were incubated with complete medium without acid treatment as a negative control. The number of viable

cells was expressed as a percentage relative to negative control. Results are mean ± standard error of the mean (SEM) of at least three independent experiments. Values significantly different from negative control: * $p<0.05$; ** $p<0.01$; *** $p<0.001$. Values significantly different from 3-BP IC_{50}: # $p<0.05$; ### $p<0.001$, One-way ANOVA and Tukey Test.

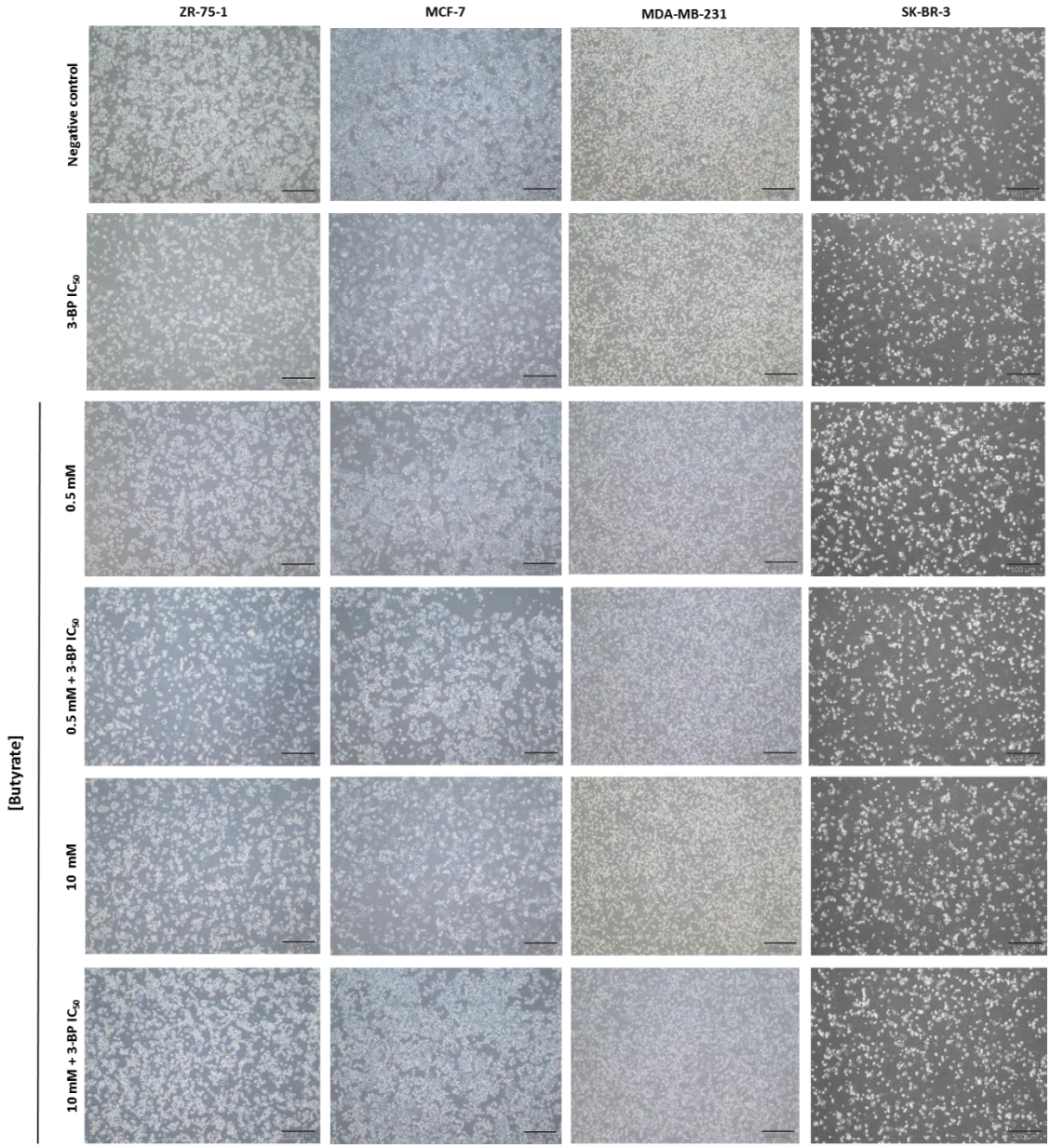

Figure 12. Analysis of cellular confluence of ZR-75-1, MCF-7, MDA-MB-231 and SK-BR-3 breast cancer cell lines at 16 hours, after treatment with butyrate (0.5 and 10 mM) alone or in combination with 3-BP IC_{50}. Negative control corresponds to cells submitted to the same conditions but without carboxylic acid treatment. Representative photos are shown. The scale bar corresponds to 500 μm.

4.3. Effect of butyrate and 3-BP treatment on MCTs expression

In order to explore whether the viability phenotypes observed were associated to the capacity of butyrate to induce MCTs expression as already described by our group (Queiros, Preto et al. 2012), cells were treated under the conditions described above for 16 hours, and the expression of MCT1, MCT2, MCT4, CD147, CD44 proteins was accessed by western blot.

For the most sensitive cell line, ZR-75-1, treatment with 3-BP IC_{50} increased MCT1, MCT2 and MCT4 protein expression compared to the negative control (Figure 13). Western blot analysis showed that 0.5 mM and 10 mM butyrate decreased the expression of MCT4 but not MCT1, MCT2 and both forms of CD147 (FG and CG) compared to negative control. Co-incubation of 0.5 mM butyrate with 3-BP IC_{50} increased the expression of MCT1, MCT2 and MCT4, while the combination of 10 mM butyrate with 3-BP IC_{50} decreased the expression levels of these proteins. Treatment with 3-BP IC_{50} alone and in co-incubation with 0.5 mM butyrate also decreased the levels of β-actin protein (Figure 13).

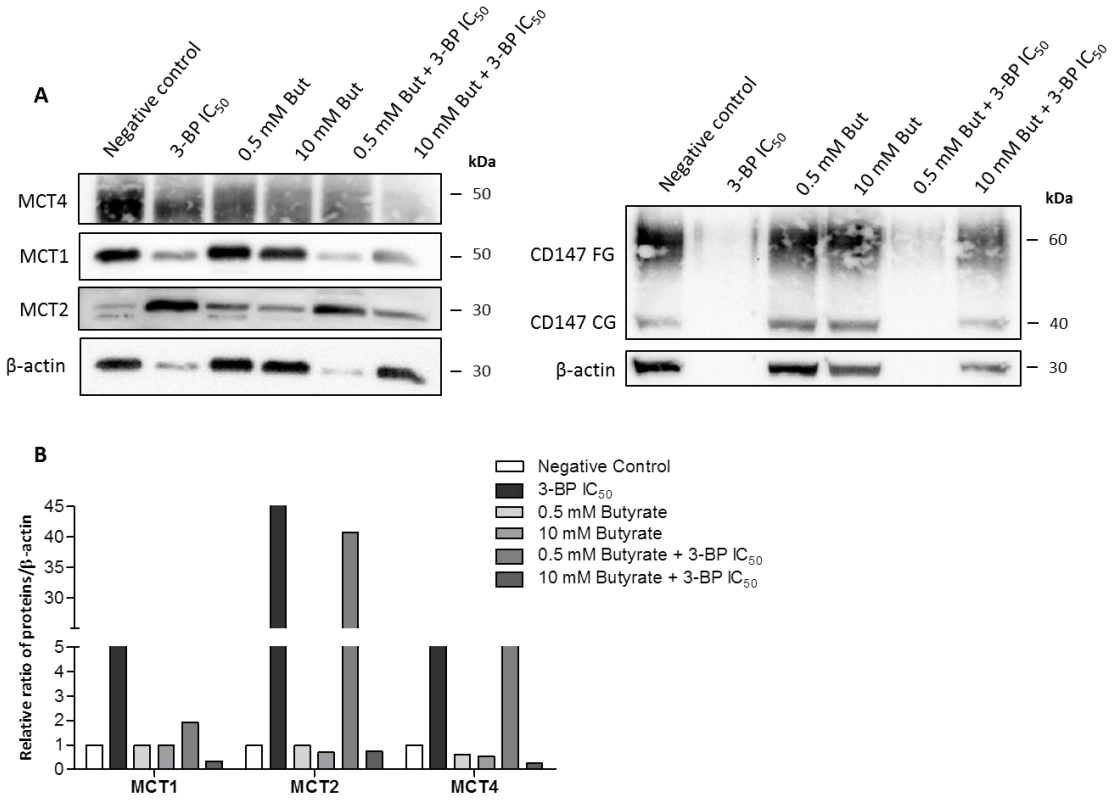

Figure 13. Expression analysis of MCT1, MCT2, MCT4 and CD147 in ZR-75-1 breast cancer cell line after treatment with butyrate (0.5 mM and 10 mM) alone or in combination with 3-BP IC_{50} for 16 hours. (A) Western blot of all proteins tested as indicated in the left part of the blots. Protein molecular

weights observed are consistent to describe for these proteins and are showed at the right of the blots. Cells were incubated with complete medium without acid treatment as a negative control. β-actin level was used as loading control. (B) Quantification of proteins levels relative to negative control. Bands were quantified in ImageJ software. FG – fully glycosylated; CG – core glycosylated

In MCF-7 cell line, the β-actin expression was not detected in untreated cells (negative control), while treatment with 0.5 mM of butyrate increased the expression of MCT4 compared to 10 mM of butyrate (Figure 14 (left panel)). Treatment with 3-BP IC_{50} alone or in combination with 0.5 mM but not 10 mM of butyrate increased the MCT2 expression and decreased the expression levels of β-actin protein (Figure 14 (right panel)). MCT1 and CD147 were not detectable after stripping of the membranes.

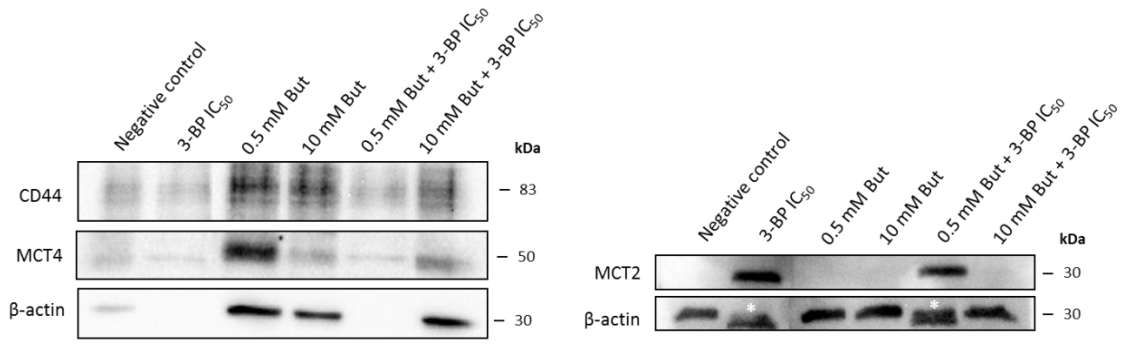

Figure 14. Expression analysis of MCT2, MCT4 and CD44 in MCF-7 breast cancer cell line after treatment with butyrate (0.5 mM and 10 mM) alone or in combination with 3-BP IC_{50} for 16 hours. Western blot of all proteins tested as indicated in the left part of the blots. Protein molecular weights observed are consistent to describe for these proteins and are showed at the right of the blots. Cells were incubated with complete medium without acid treatment as a negative control. β-actin level was used as loading control. * corresponds to the MCT2 protein band.

In MDA-MB-231 cell line, treatment with 3-BP IC_{50} increased the expression of MCT4 but not MCT1 (Figure 15). Treatment with both concentrations of butyrate (0.5 mM and 10 mM) did not alter the expression of MCT1 and MCT4, while the combination with 3-BP IC_{50} increased MCT4 and decreased MCT1 expression (Figure 15). MCT2 expression was not detected in any tested conditions (Figure 15). CD147 was not detectable after stripping of the membrane.

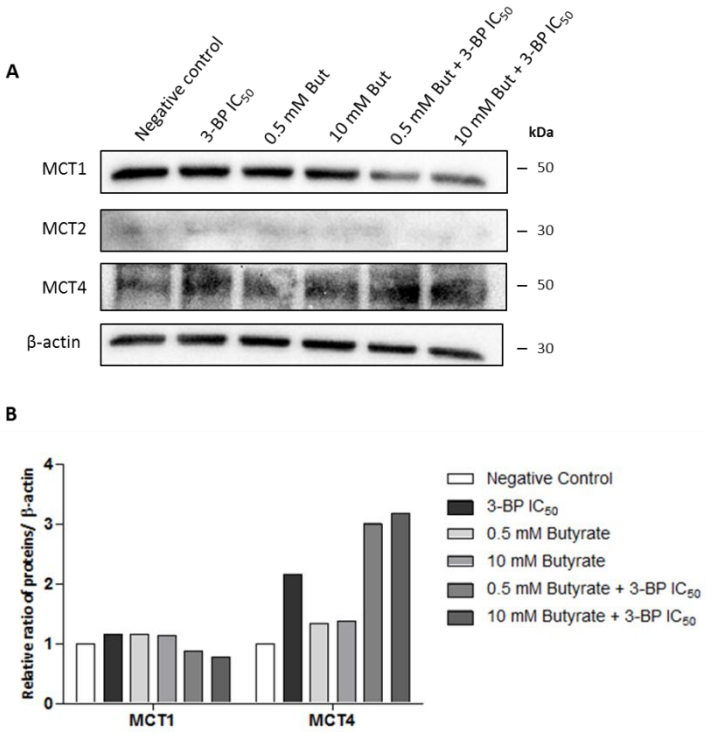

Figure 15. Expression analysis of MCT1, MCT2 and MCT4 in MDA-MB-231 breast cancer cell line after treatment with butyrate (0.5 mM and 10 mM) alone or in combination with 3-BP IC_{50} for 16 hours. (A) Western blot of all proteins tested as indicated in the left part of the blots. Protein molecular weights observed are consistent to describe for these proteins and are showed at the right of the blots. Cells were incubated with complete medium without acid treatment as a negative control. β-actin level was used as loading control. (B) Quantification of proteins levels relative to negative control. Bands were quantified in ImageJ software.

In the more resistant cells to 3-BP, SK-BR-3, MCT2 expression was not detected in any tested conditions (Figure 16). Treatment with 3-BP IC_{50} increased MCT1 and MCT4 expression, but decreased the expression of fully glycosylated (FG) form of CD147 compared to negative control. Both concentrations of butyrate (0.5 mM and 10 mM) alone or in combination with 3-BP IC_{50} increased the expression of MCT4, MCT1 and both forms of CD147 (Figure 16).

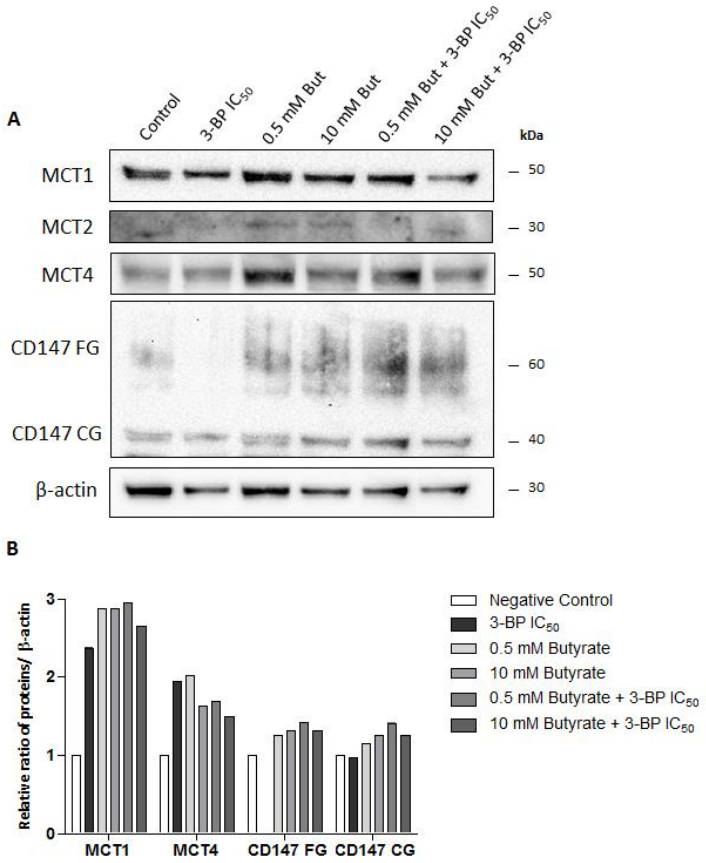

Figure 16. Expression analysis of MCT1, MCT2, MCT4 and CD147 in SK-BR-3 breast cancer cell line after treatment with butyrate (0.5 mM and 10 mM) alone or in combination with 3-BP IC_{50} simultaneously for 16 hours. (A) Western blot of all proteins tested as indicated in the left part of the blots. Protein molecular weights observed are consistent to describe for these proteins and are showed at the right of the blots. Cells were incubated with complete medium without acid treatment as a negative control. β-actin level was used as loading control. (B) Quantification of proteins levels relative to negative control. Bands were quantified in ImageJ software. FG – fully glycosylated; CG – core glycosylated

4.4. Effect of 3-BP on actin structure

The results obtained by western blot in the expression levels of actin after 3-BP treatment led us to study the effect of 3-BP on actin structure in ZR-75-1 and SK-BR-3 cell lines. For that propose, cells were treated with 3-BP in a concentration corresponding to the respective IC_{50} for each cell line, for 16 hours. After 16 hours, cells were stained with Alexa Fluor 488 Phalloidin, a fluorescent probe specific for filamentous actin (F-actin) and visualized in a fluorescence microscope (Figure 17). Our preliminary results showed that treatment with 3-BP IC_{50} seems to

reduced the amount of actin in ZR-75-1 but not in SK-BR-3 cell line, what is in according to the results of western blot for actin protein (Figure 13 and 16). For ZR-75-1 cells, 3-BP treatment also altered the actin appearance and cellular shaping of cells from elongate to round cells, while in SK-BR-3 this phenotypic alteration was not so evident (Figure 17).

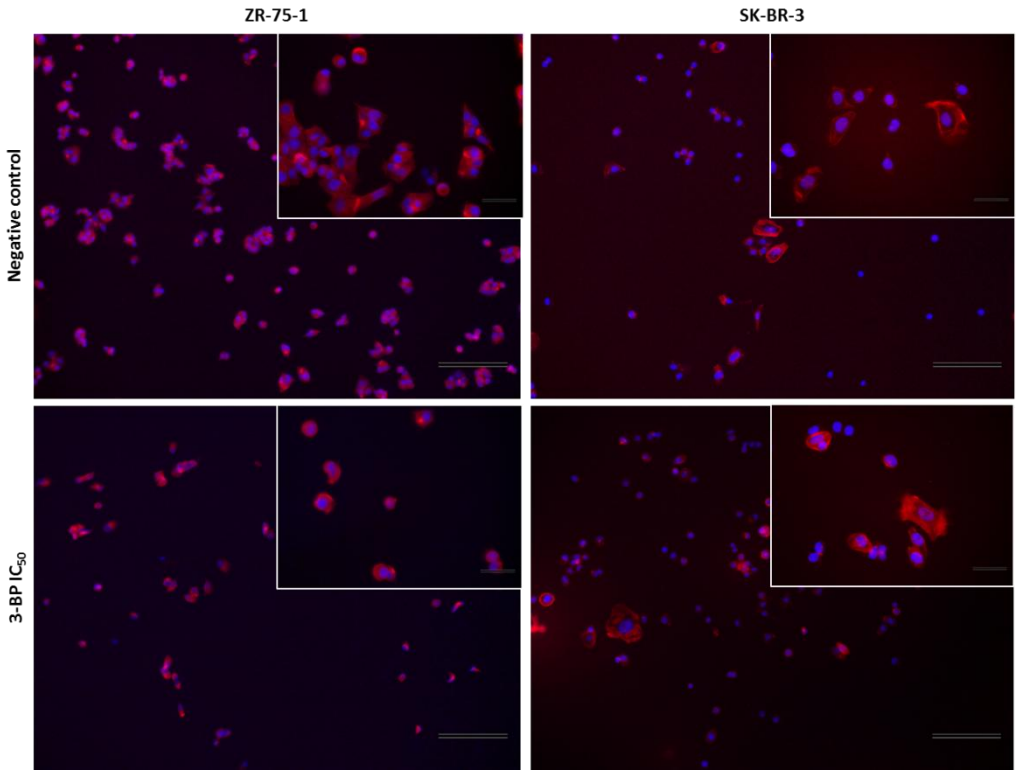

Figure 17. Actin structural alterations in ZR-75-1 and SK-BR-3 cell lines, after treatment with 3-BP IC_{50} for 16 hours. Cells were incubated with complete medium without 3-BP treatment as a negative control. Alexa Fluor 488 Phalloidin stains for F-actin in red, and DAPI stains nucleus in blue. Representative photos of two independent experiments with similar results are shown.

4.5. Optimization of MCT1 and MCT4 silencing by RNA interference

In order to determine the contribution of monocarboxylate transporters (MCTs) on butyrate and 3-BP effect in breast cancer cells, the conditions for MCT1 and MCT4 silencing by RNA interference (RNAi) were optimized. For the optimization of the reverse transfection conditions, Lipofectamine RNAiMAX was used as a vehicle capable to delivery exogenous siRNA into cells. Firstly, the initial cellular density was optimized in ZR-75-1, MCF-7 and SK-BR-3 cells for the RNAi assay. The cellular density was determined in order to ensure 80% confluence in the fourth day of

transfection. Different cellular densities for each cell line were inoculated and cellular confluence was visualized by phase contrast microscope. In ZR-75-1 and MCF-7 cell lines were determined cell density of 100 000 cells and in SK-BR-3 cell line of 50 000 cells. To ensure the best conditions for siRNA delivery with high efficiency and low cytotoxicity different quantities of lipofectamine (0.5 μl, 1 μl and 2 μl) were tested in cellular viability/cytotoxicity and in internalization capability of a non-target siRNA labeled with Alexa Fluor 488 (siRNA-AF). After four days of transfection, the cytotoxicity of Lipofectamine RNAiMAX was evaluated by trypan blue exclusion assay and the cellular uptake of siRNA-AF was accessed by fluorescence microscopy (Figure 18).

For ZR-75-1, trypan blue exclusion assay results showed that both 0.5 μl and 2 μl of Lipofectamine RNAiMAX did not altered cell viability (100%) and 1 μl of Lipofectamine RNAiMAX condition has no significant reduction on cellular viability compared to the negative control being 92% (Figure 18A). Analysis of siRNA-AF cellular uptake in ZR-75-1 indicated that 1 μl of Lipofectamine RNAiMAX presented more internalization of siRNA-AF than the other conditions (Figure 18B). In MCF-7, the Lipofectamine RNAiMAX also seems to be non-cytotoxic for cells since the percentage of viability was 100% in 0.5 μl and 1μl of Lipofectamine RNAiMAX conditions and 94% for 2 μl of Lipofectamine RNAiMAX compared to negative control. Fluorescence microscopy allowed to determine that 1 μl of Lipofectamine RNAiMAX presented more siRNA-AF located in the cellular cytoplasm than the other conditions (Figure 18B). Finally, in SK-BR-3 the trypan blue exclusion assay demonstrated that Lipofectamine RNAiMAX was not cytotoxic in all tested conditions and 2 μl of Lipofectamine RNAiMAX demonstrated the better internalization of siRNA-AF (Figure 18). The results indicated that the combination of 1 μl of Lipofectamine RNAiMAX transfection reagent with 5 nM of siRNA presented the better condition for further silencing in ZR-75-1 and MCF-7 cell lines, and the combination 2 μl of Lipofectamine RNAiMAX with 5 nM in SK-BR-3 cell line.

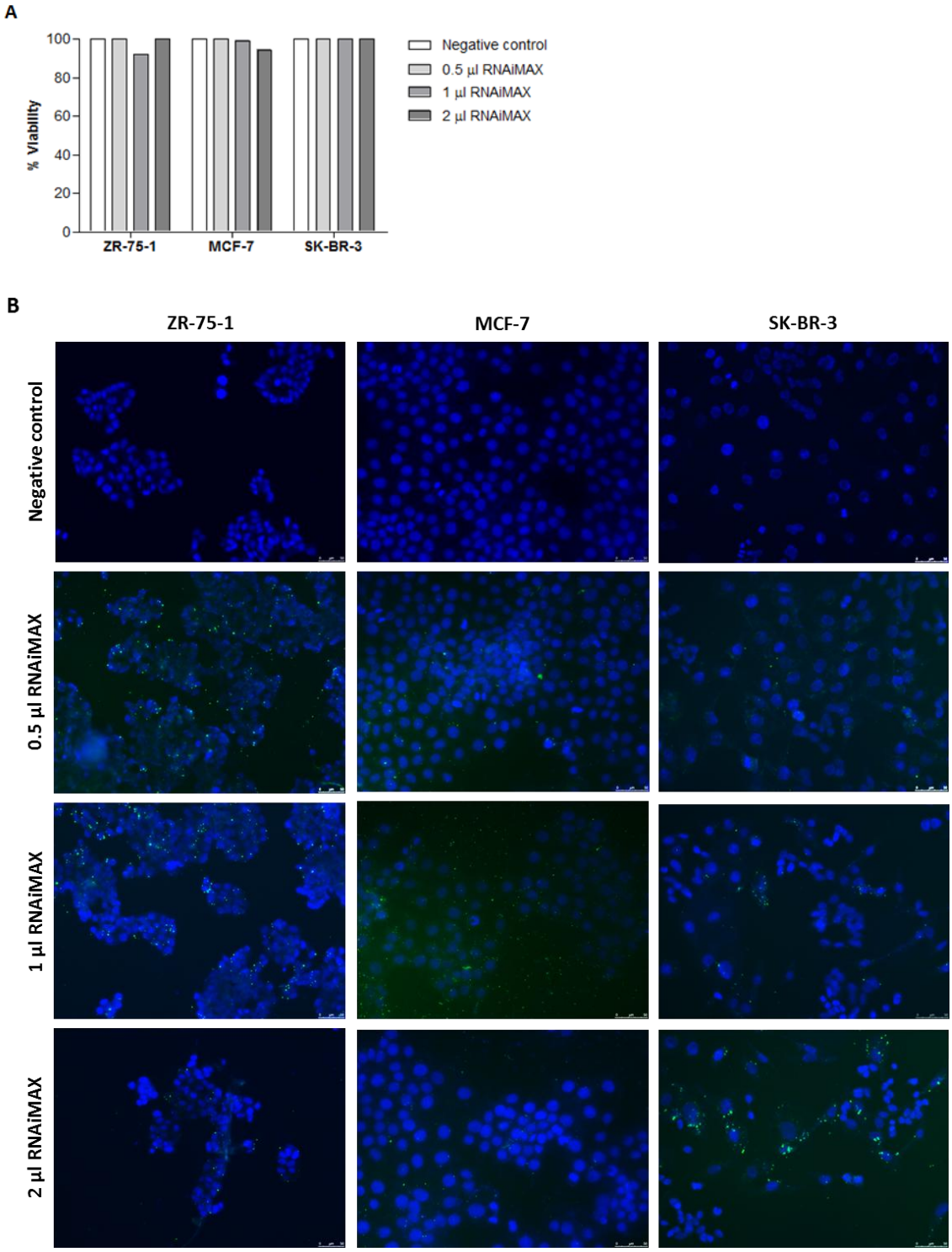

Figure 18. Optimization of RNAi reverse transfection conditions with Lipofectamine RNAiMAX transfection reagent in ZR-75-1, MCF-7 and SK-BR-3 cell lines using non-target siRNA labeled with Alexa Fluor 488 (5 nM). (A) Cell lines were transfected with 0.5 µl, 1 µl and 2 µl of Lipofectamine RNAiMAX. After 4 days, cell viability was determined by trypan blue exclusion assay and expressed as a percentage. Negative control was performed with Opti-MEM alone. (B) Cellular internalization of non-target siRNA labeled with Alexa Fluor 488 (siRNA-AF) by transfections with different quantities of Lipofectamine

RNAiMAX (0.5, 1 and 2 μl). After 4 days, siRNA-AF fluorescence (green) and nuclei stain with DAPI (blue) was visualized by fluorescence microscopy. Representative photos are shown (20x magnification).

For the optimization of MCT1 and MCT4 inhibition by RNAi we tested two different concentrations (5 nM and 10 nM) of siRNA target for MCT1 and MCT4 in ZR-75-1 and SK-BR-3 cell lines. After four and/or five days of transfection knockdown of target genes was confirmed at protein level by western blot.

In ZR-75-1 cell line, after four days of transfection with 5 nM of siRNA target MCT1 the expression of MCT1 protein decreased 2%, while with 10 nM of siRNA decreased 6%, compared to non-silencing siRNA control (siRNA control) (Figure 19). After five days of transfection with both 5 nM and 10 nM of siRNA target MCT1 the expression of MCT1 protein increased 51% and 79%, respectively compared to siRNA control (Figure 19).

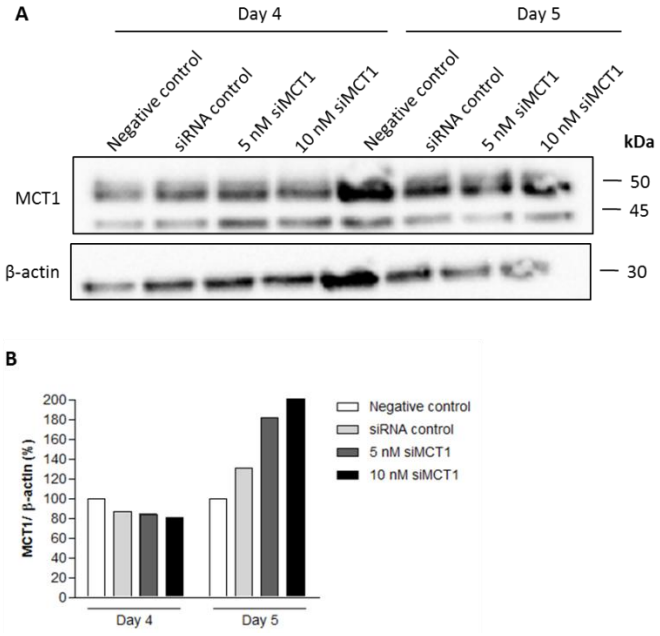

Figure 19. Expression analysis of MCT1 protein after siRNA-mediated silencing with siRNA target MCT1 in ZR-75-1 breast cancer cell line in the fourth and fifth days of transfection. (A) Western blot of MCT1 as indicated in the left part of the blot. Protein molecular weight observed is consistent to describe for this protein and is showed at the right of the blot. β-actin level was used as loading control. Negative control was performed with Opti-MEM alone and siRNA control was performed with non-silencing siRNA. (B) Quantification of proteins levels relative to negative control in the fourth and fifth day of silencing. Bands were quantified in ImageJ software.

The western blot analysis of silencing with siRNA target MCT4 in ZR-75-1 cell line showed that in the fourth day of transfection 5 nM of siRNA MCT4 increased 16% of MCT4 protein expression, while 10 nM of siRNA MCT4 decreased 12% of MCT4 expression, compared to non-silencing siRNA control (siRNA control) (Figure 20). After five days of transfection with both 5 nM and 10 nM of siRNA MCT4 reduced 20% of MCT4 protein expression, compared to siRNA control (Figure 20).

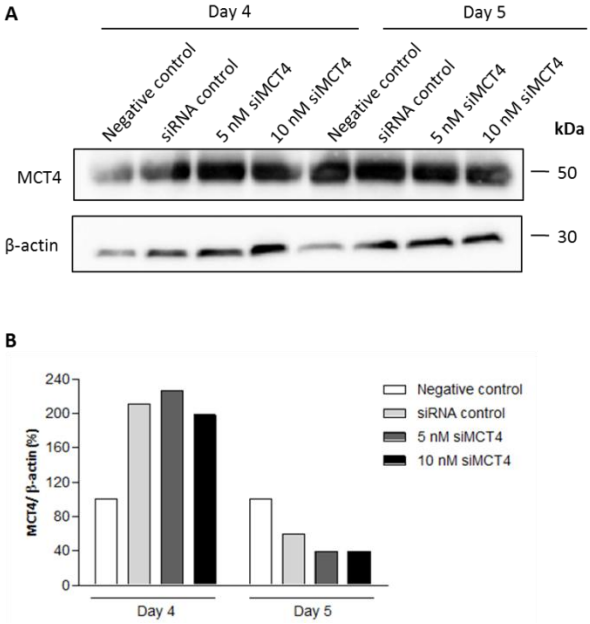

Figure 20. Expression analysis of MCT4 protein after siRNA-mediated silencing with siRNA target MCT4 in ZR-75-1 breast cancer cell line in the fourth and fifth days of transfection. (A) Western blot of MCT4 as indicated in the left part of the blot. Protein molecular weight observed is consistent to describe for this protein and is showed at the right of the blot. β-actin level was used as loading control. Negative control was performed with Opti-MEM alone and siRNA control was performed with non-silencing siRNA. (B) Quantification of proteins levels relative to negative control in the fourth and fifth day of silencing. Bands were quantified in ImageJ software.

In the SK-BR-3 cell line, western blot analysis of silencing with siRNA target MCT1 showed that, transfection with 5 nM of siRNA MCT1 decreased 17.7% of MCT1 protein expression, while 10 nM of siRNA MCT1 decreased 28.8% of MCT1 expression compared to the non-silencing siRNA control, after five days of transfection (Figure 21). The transfection with non-silencing siRNA control (siRNA control) decreased 60% of MCT1 protein expression compared to the negative control.

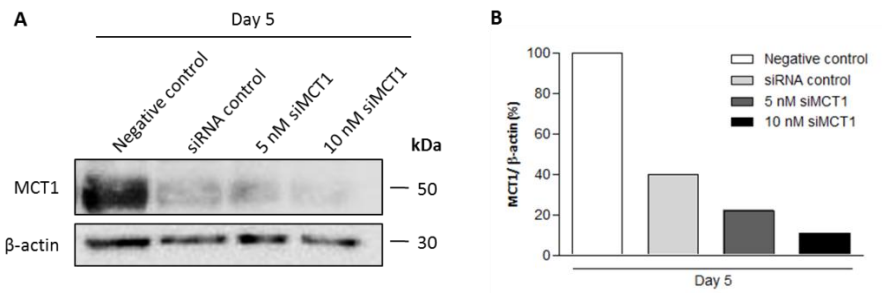

Figure 21. Expression analysis of MCT1 protein after siRNA-mediated silencing with siRNA target MCT1 in SK-BR-3 breast cancer cell line in the fifth day of transfection. (A) Western blot of MCT1 as indicated in the left part of the blot. Protein molecular weight observed is consistent to describe for this protein and is showed at the right of the blot. β-actin level was used as loading control. Negative control was performed with Opti-MEM alone and siRNA control was performed with non-silencing siRNA. (B) Quantification of proteins levels relative to negative control in the fifth day of silencing. Bands were quantified in ImageJ software.

The western blot analysis of silencing with siRNA target MCT4 in SK-BR-3 cell line revealed that transfection with 5 nM of siRNA MCT4 decreased 71% of MCT4 protein expression, while 10 nM of siRNA MCT4 decreased 66% of MCT4 expression compared to non-silencing siRNA control (Figure 22). We also evaluated whether the down-regulation of MCT4 in these conditions led to alterations in expression levels of MCT1 and ancillary proteins CD44/CD147 (Figure 22). Western blot analysis of MCT4 silencing showed that 10 nM of siRNA MCT4 decreased 46% of MCT1 and 50% of CD44 expression compared to the non-silencing siRNA control. Treatment with 5 nM of siRNA MCT4 decreased 17% of fully glycosylate (FG) form of CD147, while treatment with 10 nM of siRNA MCT4 decreased 96%, compared to non-silencing siRNA control.

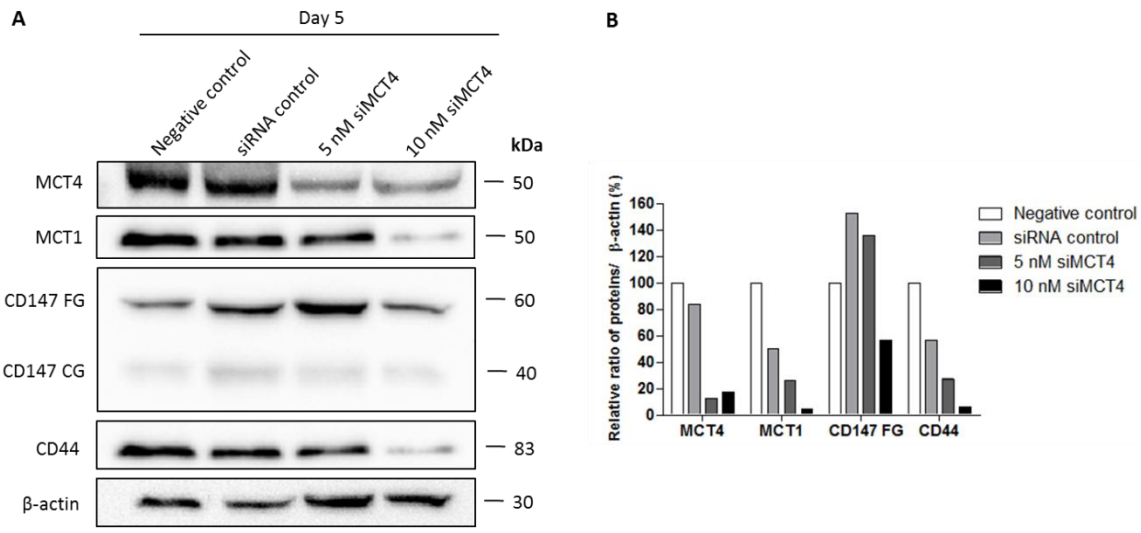

Figure 22. Expression analysis of MCT1, MCT4 and CD147 after siRNA-mediated silencing with siRNA target MCT4 in SK-BR-3 breast cancer cell line in the fifth day of transfection. (A) Western blot of MCT1, MCT4 and CD147 as indicated in the left part of the blot. Protein molecular weights observed are consistent to describe for these protein and are showed at the right of the blot. β-actin level was used as loading control. Negative control was performed with Opti-MEM alone and siRNA control was performed with nonsilencing siRNA. (B) Quantification of proteins levels relative to negative control in the fifth day of silencing. Bands were quantified in ImageJ software.

4.6. Effect of butyrate and 3-BP treatment on the cell cycle

To evaluate the effect of butyrate alone or in combination with 3-BP on the cell cycle, exponentially growing cells were treated as described above for 16 hours and the cell cycle distribution was determined by flow cytometry using propidium iodide (PI) as a probe for DNA.

Cell cycle analysis showed that, after 16 hours, ZR-75-1, MCF-7 and SK-BR-3 cell lines exhibited a higher percentage of cells with sub-G1 DNA content in negative control, indicative of higher cell death. Moreover, cells with G2 and S DNA content were not possible to identify in the histograms of these cell lines (data not showed).

In MDA-MB-231 cells, treatment with 3-BP IC_{50} alone did not altered the percentage of cells with G1 DNA content (31%), S DNA content (44%) and G2 DNA content (26%) compared to negative control (Figure 23A and 23B). Lower concentration of butyrate (0.5 mM) alone or in combination with 3-BP IC_{50} did not altered the percentage of cells with G1 DNA content relative to negative control being approximately 31%, while only the co-incubation of 0.5 mM butyrate with

3-BP IC_{50} decreased the percentage of cells with G2 DNA content from 22% to 8%, compared to negative control. Treatment with 10 mM of butyrate alone or in combination with 3-BP IC_{50} increased the percentage of cells with G1 DNA content to 52% and 51%, respectively, compared to negative control (32%) (Figure 23A and 23B). Moreover, treatment with 10 mM of butyrate alone or in combination with 3-BP IC_{50} decreased the percentage of cells with S phase DNA content from 46% (negative control) to approximately 40%, while the percentage of cells with G2 DNA decreased from 22% (negative control) to 9% and 11%, respectively (Figure 23A and 23B). Treatment with 3-BP IC_{50} alone, increased the percentage of cells with less than normal amount of DNA content (sub-G1 DNA content) from 2% to 4%, compared to negative control (Figure 23C). Lower concentration of butyrate (0.5 mM) alone or in combination with 3-BP IC_{50} did not altered the percentage of cells with sub-G1 DNA content being 2% and 3% respectively, compared to negative control. Higher concentration of butyrate (10 mM) alone or in combination with 3-BP IC_{50} increased the sub-G1 population to 5% and 4%, respectively compared to negative control (Figure 23C).

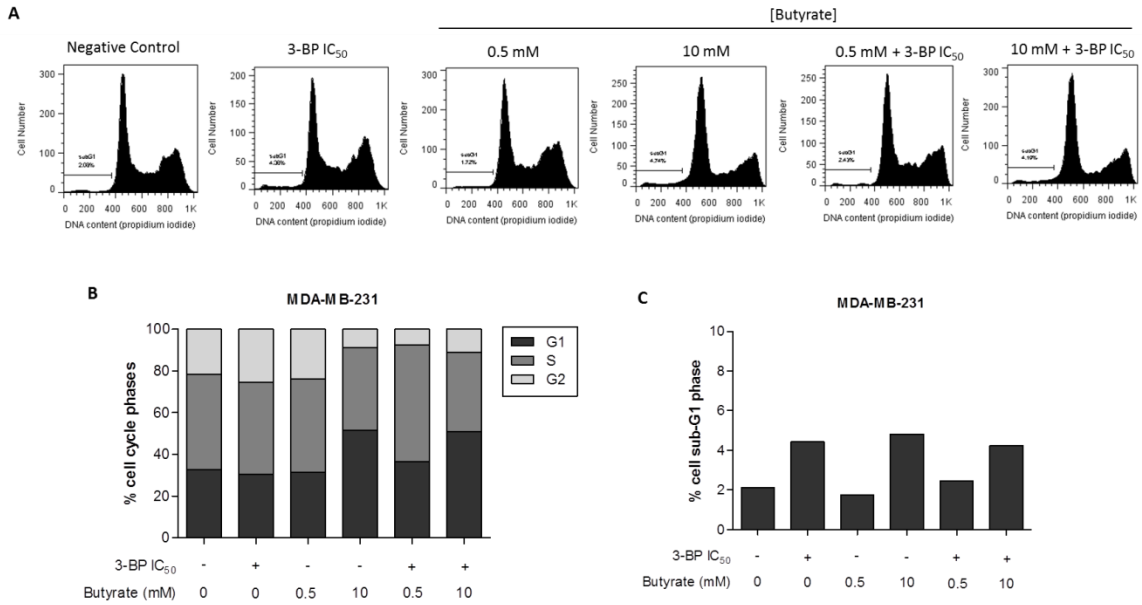

Figure 23. Analysis of the effect of butyrate (0.5 and 10 mM) alone or in combination with 3-BP IC_{50} on cell cycle of MDA-MB-231 breast cancer cell line, after 16 hours by flow cytometry. (A) Representative monoparametric histograms of DNA (number of cells versus relative DNA content) of indicated cell lines after staining with propidium iodide (PI). Cells were incubated with complete medium without acid treatment as a negative control. (B) Percentage of cells distribution of cell-cycle phases (G1, S, G2). (C) Percentage of cells with sub-G1 DNA content (cells with less than normal amount of DNA content).

5. Discussion

Reprogramming of cellular energy metabolism is an emerging hallmark of invasive carcinoma (Hanahan and Weinberg 2011). Carcinogenesis process has been associated with upregulation of metabolic pathways, mainly glycolysis. Cancer cells that exhibit Warburg effect depend on glycolysis for the production of ATP even in aerobic conditions. The export of accumulated lactate across the plasma membrane is mediated by MCTs upregulated in cancer cells, thereby protecting themselves from intracellular acidification. Given the importance of glycolysis in the tumor context, metabolic anticancer strategies are being explored. 3-BP is an alkylating agent able to inhibit metabolic pathways, namely glycolysis and oxidative phosphorylation, decreasing the production of ATP and causing cell death specifically in cancer cells (Ko, Pedersen et al. 2001). Breast cancer is the most common and lethal tumor in women worldwide, in which ER (-) breast cancers are known to be more aggressive, highly hormonal therapy resistance and associate with worse prognosis (Jemal, Bray et al. 2011). Thus, the identification of new therapeutic strategies is crucial. In the present work, the effect of butyrate alone or in combination with 3-BP in four human breast cancer cell lines were evaluated.

5.1. MCTs basal expression profile

In the present work, the expression profile of proteins involved in the transport of monocarboxylic acids was assessed by western blot, in four human breast cancer cell lines. All cell lines showed different basal expression profile of MCTs and ancillary proteins essential to their function. MCT1 expression was detected in two luminal subtype cell lines (ZR-75-1 (ER+) and MCF-7 (ER+)) and in subtype HER^{2+} (SK-BR-3 (ER-)) as described by Queirós and colleagues in immunohistochemistry studies (Queiros, Preto et al. 2012). The basal-like subtype MDA-MB-231 (ER-) also showed expression of MCT1, our results are not according to what has been previously reported showing that MCT1 is not expressed in this cell line, since alteration in the gene promoter results in loss of protein expression (Asada, Miyamoto et al. 2003; Hussien and Brooks 2011). In this study the evaluation of MCT2 expression was not performed since it was not detected in ZR-75-1, MCF-7 and SK-BR-3 cell lines in a previous immunohistochemistry study (Queiros, Preto et al. 2012). In addition, MCT3 expression was not assessed since its localization is specific to retinal pigment epithelium (RPE) and choroid plexus epithelia (CPE) (Halestrap 2012; Halestrap and Wilson 2012). The isoform MCT4 was highly expressed in ZR-75-

1 and MDA-MB-231 as verified by Gallagher and colleagues (Gallagher, Castorino et al. 2007), while MCF-7 and SK-BR-3 cell lines showed low MCT4 expression as already described (Queiros, Preto et al. 2012). The correct targeting and anchoring of functional MCT1 and MCT4 to the plasma membrane depends on association with chaperone CD147 in the endoplasmatic reticulum (Kirk, Wilson et al. 2000; Nabeshima, Iwasaki et al. 2006; Halestrap and Wilson 2012). Another chaperon, CD44, was also been associated to MCT plasma membrane localization (Slomiany, Grass et al. 2009; Pinheiro, Reis et al. 2010). Therefore, we also evaluate the expression profile of these ancillary proteins. CD147 was highly expressed in ZR-75-1 cell line that also expressed MCT4 and MCT1 isoforms, while CD44 was highly expressed in ZR-75-1 and MCF-7 cell lines. pH regulators systems are also involved in high glycolytic phenotype of cancer cells, thus we evaluated the expression of anion exchanger 1 (AE1) in all breast cancer cell lines. AE1 or band 3 protein was only expressed in ZR-75-1 and MCF-7. Our results indicate that the expression pattern of MCTs is not correlated with ER expression, although the cell line more aggressive SK-BR-3 (ER-) has lower expression of these transporters. Characterization of MCTs protein expression in isolated plasma membranes and organelles, such as mitochondria may add new information important to determine the distribution and localization of these transporters in cellular environment. Evaluation of other relevant proteins in cancer cell metabolism, such as HKII and GAPDH would be also important in the context of the present study giving new insights to understand the reasons why these different cell lines have different sensibilities to 3-BP.

5.2. Lower dose of butyrate potentiates the effect of 3-BP in cell lines more sensitive

The effect of butyrate alone or in combination with 3-BP on cell viability in human breast cancer cell lines was evaluated by Trypan Blue exclusion assay. The conventional assay MTT and MTS based on metabolic reduction of compounds is not so adequate when metabolism is altered (Mathupala, Parajuli et al. 2004; Ganapathy-Kanniappan, Geschwind et al. 2010). Trypan Blue exclusion assay results showed different effects on cell viability in response to butyrate alone or in co-incubation with 3-BP in all breast cancer cell lines. Butyrate decreased cell viability according to its concentration as verified by Queirós and colleagues (Queiros, Preto et al. 2012). This cytotoxic effect was more evident in cell lines more sensitive to 3-BP (ZR-75-1, MCF-7) and in

MDA-MB-231 where the lower dose of butyrate (0.5 mM) did not alter cell viability, whereas the highest dose (10 mM) decreased cell viability. In cells more resistant to 3-BP, SK-BR-3, butyrate decreased cell viability independently of dose used. The transport of anionic form of butyrate is mediated by MCT1 and SMCT1 (Cuff, Dyer et al. 2005; Gupta, Martin et al. 2006; Thangaraju, Cresci et al. 2008) and MCT1 was expressed in all breast cancer cell lines. In addition, the fact that butyrate can function at low levels as a histone acetyltransferase (HAT) promoter, influencing cell proliferation and at high levels as a histone deacetylase (HDAC) inhibitor, inducing the expression of genes that inhibit cell proliferation and promote apoptosis, probably explain the observed viability phenotypes (Donohoe, Collins et al. 2012). As verified by others in colon adenocarcinoma cells, butyrate can inhibit proliferation and induce cell death related to its function as HDAC (Hinnebusch, Meng et al. 2002). It would be interesting to evaluate the HDAC activity to ascertain if induction of cell death by higher dose of butyrate (10 mM) was associated with inhibition of HDAC in breast cancer cell lines.

The cellular response to treatment with butyrate in combination with 3-BP showed different results from our previous published results, where butyrate pre-treatment sensitized SK-BR-3 cells to 3-BP action (Queiros, Preto et al. 2012). Results of simultaneous treatment in SK-BR-3 did not potentiates the effect of 3-BP, the differences observed may be due to the time of incubation (16 hours) different from our previous published results where cells were incubated during 24 hours in medium containing butyrate followed by 16 hours incubation in medium with 3-BP. The fact that in our previous study were used MTT assay to determine cell viability, a not so adequate assay when MCT activity is altered, can also contribute to the different viability phenotypes observed in SK-BR-3 cell line.

In ZR-75-1 and MCF-7 cells, more sensitive to 3-BP, cell viability was increased in response to simultaneous treatment of 3-BP with the highest dose of butyrate, inhibiting the cytotoxic effect of 3-BP. In contrast, simultaneous treatment of 3-BP with the lower dose of butyrate decreased cell viability contributing to the 3-BP cytotoxic effect. Others studies also demonstrated the synergetic effect of lower dose of butyrate (0.5 mM) and the anticancer agent cisplatin in HeLa cells after 1 day of treatment (Koprinarova, Markovska et al. 2010).

In MDA-MB-231 cell line, cell viability was decreased in response to simultaneous treatment of 3-BP with the highest dose of butyrate, contributing to cytotoxic effect of 3-BP. The mechanism for the entry of 3-BP and anionic form of butyrate involves MCT1 (Cuff, Dyer et al. 2005; Birsoy, Wang et al. 2013), the affinity of substrates for MCT1, may be explain these

results. Complemented radioactivity studies with 3-BP and butyrate radiolabelled would be important to explore these results based on entry of 3-BP and butyrate into cancer cells.

5.3. 3-BP induces MCT2 expression in cell lines more sensitive

We hypothesized that butyrate possibly regulate the expression of monocarboxylate transporters in co-treatment with 3-BP contributing to its cytotoxicity effect. In order to explore the different viability phenotypes observed, MCTs expression was assessed by western blot in all cell lines upon carboxylic acid treatment. We observed that 3-BP increased the expression of MCT2 in the most sensitive cell lines, ZR-75-1 and MCF-7 and moreover, the high expression of MCT2 was also detected in co-treatment with the lower dose of butyrate but not with the higher dose.

In ZR-75-1, treatment with 3-BP alone or in combination with the lower dose of butyrate (0.5 mM) increased the expression of MCT1, MCT2 and MCT4, while in combination with the higher dose decreased the expression of these MCTs isoforms. Maintenance of MCTs expression pattern upon treatment with 3-BP alone or in combination with a lower dose of butyrate could be related to the cytotoxic effect on cell viability described. MCT2 catalyzes with higher affinity the uptake of lactate and pyruvate in gluconeogenic cells such localized in brain and liver (Halestrap and Meredith 2004). The upregulation of MCT2 by 3-BP suggests that this MCT isoform could have an important function some organelle membranes. McClelland and colleagues demonstrated a possible role of MCT2 in hepatocyte peroxisomal membrane (McClelland, Khanna et al. 2003). Evaluation of the MCT2 localization in the cell by immunocytochemistry or analysis of protein expression in isolated organelles membranes by western blot would be necessary to determine the involvement of this MCT isoform in 3-BP cytotoxic effect.

In MCF-7 cell line, treatment with higher dose of butyrate decreased the expression of MCT4. In contrast treatment with butyrate alone or in combination with 3-BP increased the expression of MCT4 but not MCT1 in MDA-MB-231 cell line. In more resistant cells SK-BR-3, the expression of MCT1, MCT2 and MCT4 was not induced by 3-BP and lower doses of butyrate (0.5 mM) alone or in combination with 3-BP induced the expression of MCT4 but not MCT1 as previous verified by us in immunohistochemistry studies (Queiros, Preto et al. 2012). The affinity of butyrate and 3-BP to MCT1 could explain the different phenotype observed with low and high dose of butyrate.

5.4. 3-BP reduces the amount of actin in most sensitive cell line

In this work, actin protein was not detected by western blot upon 3-BP treatment in the cell lines more sensitive to 3-BP, ZR-75-1 and MCF-7. Therefore, we investigated if 3-BP could induce alterations in actin structure by fluorescence microscopy using Alexa Fluor 488 Phalloidin, a fluorescent probe with high affinity to filamentous actin (F-actin). Our preliminary results showed that 3-BP reduced the amount of actin in ZR-75-1 but not in the most resistant cell line, SK-BR-3. Moreover, the shape of ZR-75-1 but not SK-BR-3 cells was also altered from elongate to round cells. F-actin cytoskeleton lost its stress fibers and adopted a more rounded morphology, after 16 hours of treatment with 3-BP in ZR-75-1 cell line. These results could suggest that 3-BP action also affects actin dynamics recently associated with the phenomenon termed anoikis, characterized by loss of attachment to the extracellular matrix and consequent apoptosis (Frisch and Screaton 2001). Cancer cells resistant to anoikis after cell detachment which contributes to metastasis allowing cancer cells invade distant sites (Simpson, Anyiwe et al. 2008). This resistance is promoted by activation of survival pathways such as induced by PI3K signaling and HIF-1, also important in maintenance of glycolysis (Rohwer, Welzel et al. 2008). Recent study showed that treatment with an inhibitor of histone deacetylase activity (HDAC), SAHA, restores sensitivity to anoikis in MDA-MB-231 breast cancer cells (Lauricella, Ciraolo et al. 2011). Our preliminary results suggest that 3-BP could induce cell death by anoikis in more sensitive cell line ZR-75-1. However, these results need further confirmation, as well as validation through a anoikis assay to ascertain if 3-BP induced cell death in ZR-75-1 by this apoptotic pathway, such a cell detachment assay in a poly-HEMA-coated plates. Invasion and migration are important mechanisms in tumor progression allowing cancer cells to escape from primary tumor and colonize other regions (Hanahan and Weinberg 2011). Evaluate the influence of 3-BP in migration and invasion capacity by wound-healing assay and matrigel invasion assay, would be also important to explore the mechanism of action of this anticancer drug.

5.5. Optimization of RNAi conditions for MCT1 and MCT4 silencing

In order to explore the role of MCTs in butyrate and 3-BP cytotoxic effect, the conditions for MCT1 and MCT4 silencing by RNA interference (RNAi) were optimized in ZR-75-1, MCF-7 and SK-

BR-3 cell lines. The transfection conditions were not optimized for MDA-MB-231 cell line since the inhibition of MCT4 expression by RNAi is described in the literature (Gallagher, Castorino et al. 2007). Transfection reagent Lipofectamine RNAiMAX was efficient in delivery exogenous fluorescent non-target siRNA (siRNA-AF) with low cytotoxicity in all cell lines after four days of transfection. In ZR-75-1 and MCF-7 cell lines, 1 μl of Lipofectamine RNAiMAX presented more internalization of siRNA-AF. Moreover, in SK-BR-3, 2 μl of Lipofectamine RNAiMAX was more efficient in cellular delivery of siRNA-AF. The amount of specific siRNA target MCT1 and MCT4 and time point were also optimized for ZR-75-1 and SK-BR-3 cell lines. In ZR-75-1 cell line, inhibition of MCT4 and MCT1 expression with both 5 nM and 10 nM siRNA target resulted in very lower silencing of the two proteins after 4 and 5 days of transfection. In SK-BR-3, the transfections showed inefficient in specific MCT1 silencing since transfection with non-silencing siRNA resulted in downregulation of MCT1 expression. In fact, the transfection with non-silencing siRNA was used as a control of transfection, and since this sequence is not specific for silencing MCT1 mRNA the results of silencing of MCT1 by transfection with siRNA target MCT1 could be induced by deregulation of transcription. The inhibition of MCT4 expression with 5 nM and 10 nM siRNA target MCT4 resulted in approximately 70% reduction of protein expression in SK-BR-3 cell line. It would be important to evaluate changes in MCT1 and MCT4 mRNA levels after target silencing by RT-PCR, to confirm silencing. In addition, it would be also interesting to performe also MCTs activity inhibition with specific inhibitors of MCTs such as developed by AstraZeneca to ascertain the involvement of MCTs activity in butyrate and 3-BP cytotoxic effect.

5.6. Highest dose of butyrate increases the number of cells on G1 phase in MDA-MB-231 cell line

To evaluate the effect of butyrate alone or in combination with 3-BP on cell cycle, a flow cytometry analysis by measuring the DNA content of cells was performed.

Cell cycle is a series of ordered events that leads to cell's division and duplication. These events comprise interphase, mitosis and cytokinesis. The interphase consist in three phases, where G1 phase (Gap 1) is responsible for cell growth, mRNA and proteins synthesis required for DNA replication, S phase (DNA synthesis) in which DNA replicates followed by G2 phase (Gap 2) wherein cell prepares to divide in mitosis process. After interphase, cell cycle proceeds to mitotic

phase defined by mitosis and cytokinesis. Mitosis (M phase) is the nuclear division and comprises prophase, metaphase, anaphase and telophase and the cytokinesis is the cytoplasmatic division. Cell cycle analysis performed by flow cytometry using propidium iodide (PI), a fluorescent dye that intercalates DNA allowing a precise measurement of DNA content of cells in different phases of interphase, including sub-G1 assumed as death cells.

In the present work, the highest dose of butyrate (10 mM) alone or in co-incubation with 3-BP IC_{50} increased the percentage of cells in G1 phase, in MDA-MB-231 cells. In fact, other study showed that 10 mM of butyrate affects cell cycle at very early stage of G1 phase in Madin Darby Bovine Kidney cells (MDBK) (Li 2011). Moreover, 10 mM butyrate alone or in combination with 3-BP increased the percentage of cells with sub-G1 DNA content may be due to the DNA fragmentation in death cells suggesting that apoptosis might occur. The flow cytometry analysis confirmed the results of trypan blue exclusion assay. However, more studies are need to better understand the role of butyrate alone or in combination with 3-BP in MDA-MB-231 cell cycle since these results were obtained from a single experiment. Concerning the other cell lines higher percentage of cells with sub-G1 DNA content without acid treatment were observed, not being possible to distinguish the cell cycle phases G1, S and G2 in the monoparametric histograms of DNA. The fact that adherent cells need to be trypsinized or scraped to prepare individual cells in suspension to be analyzed by flow cytometry, promote loss of membrane integrity and consequent entry of PI into the cells. It would be necessary to optimize this critical point of protocol and cytometer parameters as intensity of fluorescence (FL-3 channel (488/620 nm)) to ascertain the effect of butyrate and 3-BP in ZR-75-1, MCF-7 and SK-BR-3 cell lines on cell cycle. Additional assays, such as Annexin/PI assay, western blot analysis of activated caspase-3, or TUNEL assay indicative of apoptosis, would be necessary to determine which type of cell death is being triggered: apoptosis or necrosis.

6. Final Remarks and Future Perspectives

Carcinogenesis is a multistage process marked by the reprograming of cellular energy metabolism of cancer cells (Hanahan and Weinberg 2011). MCTs are key players in high glycolytic metabolism and acid resistant phenotype allowing the efflux of formed lactate couple to the output of a proton (Chiche, Brahimi-Horn et al. 2010). 3-BP is pyruvate analogue, and an alkylating agent able to inhibit the energetics of cancer cells (Ko, Pedersen et al. 2001). In the present study we intent elucidated the mechanism of 3-BP action in the presence of a monocarboxylic acid butyrate. Our observations indicated that four human breast cancer cell lines presented a distinct basal expression pattern of MCTs and ancillary proteins important to their function. The different expression of MCTs should be taken into account given the importance of these transporters in the selective effect of 3-BP.

Our results showed that lower dose of butyrate contribute to cytotoxic effect of 3-BP, while the high dose led to an inhibition effect in the more sensitive human breast cancer cell lines, ZR-75-1 and MCF-7. In addition, we also found that 3-BP alone or in combination with the lower dose of butyrate induced the expression of MCT2 in ZR-75-1 and MCF-7. Understanding the role of MCTs in 3-BP cytotoxic effect may be a starting point to uncover selective process of 3-BP uptake into cancer cells. Thus, we started to optimize the conditions for siRNA-mediated silencing of MCT1 and MCT4 expression in breast cancer cell lines to explore the results.

In this work we also observed that 3-BP induced alteration in actin structure in ZR-75-1, feature associated to cell death induced by anoikis. However, for the complete understanding of this mechanism additionally experiments are necessary. Other important question that needs to be answered is the effect of 3-BP alone or in combination with butyrate in non-tumorigenic human mammary epithelial cells, such as in MCF-10A cell line. It would be also interesting to study the effect of 3-BP in animal breast cancer models (e. g. mice) since *in vitro* studies do not mimic all tumor conditions.

7. References

Acan, N. L. and N. Ozer (2001). "Modification of human erythrocyte pyruvate kinase by an active site-directed reagent: bromopyruvate." J Enzyme Inhib **16**(5): 457-64.

Agrawal, N., P. V. Dasaradhi, et al. (2003). "RNA interference: biology, mechanism, and applications." Microbiol Mol Biol Rev **67**(4): 657-85.

Al-Ejeh, F., C. E. Smart, et al. (2011). "Breast cancer stem cells: treatment resistance and therapeutic opportunities." Carcinogenesis **32**(5): 650-8.

Asada, K., K. Miyamoto, et al. (2003). "Reduced expression of GNA11 and silencing of MCT1 in human breast cancers." Oncology **64**(4): 380-8.

Bergersen, L., E. Johannsson, et al. (1999). "Cellular and subcellular expression of monocarboxylate transporters in the pigment epithelium and retina of the rat." Neuroscience **90**(1): 319-31.

Birsoy, K., T. Wang, et al. (2013). "MCT1-mediated transport of a toxic molecule is an effective strategy for targeting glycolytic tumors." Nat Genet **45**(1): 104-8.

Blessinger, K. J. and G. Tunnicliff (1992). "Kinetics of inactivation of 4-aminobutyrate aminotransferase by 3-bromopyruvate." Biochem Cell Biol **70**(8): 716-9.

Bonnet, S., S. L. Archer, et al. (2007). "A mitochondria-K+ channel axis is suppressed in cancer and its normalization promotes apoptosis and inhibits cancer growth." Cancer Cell **11**(1): 37-51.

Boren, J., M. Cascante, et al. (2001). "Gleevec (STI571) influences metabolic enzyme activities and glucose carbon flow toward nucleic acid and fatty acid synthesis in myeloid tumor cells." J Biol Chem **276**(41): 37747-53.

Borthakur, A., S. Priyamvada, et al. (2012). "A novel nutrient sensing mechanism underlies substrate-induced regulation of monocarboxylate transporter-1." Am J Physiol Gastrointest Liver Physiol **303**(10): G1126-33.

Borthakur, A., S. Saksena, et al. (2008). "Regulation of monocarboxylate transporter 1 (MCT1) promoter by butyrate in human intestinal epithelial cells: involvement of NF-kappaB pathway." J Cell Biochem **103**(5): 1452-63.

Brahimi-Horn, M. C., J. Chiche, et al. (2007). "Hypoxia signalling controls metabolic demand." Curr Opin Cell Biol **19**(2): 223-9.

Broer, S., A. Broer, et al. (1999). "Characterization of the high-affinity monocarboxylate transporter MCT2 in Xenopus laevis oocytes." Biochem J **341 (Pt 3)**: 529-35.

Buijs, M., J. A. Vossen, et al. (2009). "Specificity of the anti-glycolytic activity of 3-bromopyruvate confirmed by FDG uptake in a rat model of breast cancer." Invest New Drugs **27**(2): 120-3.

Cao, X., L. Fang, et al. (2007). "Glucose uptake inhibitor sensitizes cancer cells to daunorubicin and overcomes drug resistance in hypoxia." Cancer Chemother Pharmacol **59**(4): 495-505.

Chen, Z., H. Zhang, et al. (2009). "Role of mitochondria-associated hexokinase II in cancer cell death induced by 3-bromopyruvate." Biochim Biophys Acta **1787**(5): 553-60.

Chiche, J., M. C. Brahimi-Horn, et al. (2010). "Tumour hypoxia induces a metabolic shift causing acidosis: a common feature in cancer." J Cell Mol Med **14**(771-94).

Coles, L., J. Litt, et al. (2004). "Exercise rapidly increases expression of the monocarboxylate transporters MCT1 and MCT4 in rat muscle." J Physiol **561**(Pt 1): 253-61.

Côrte-Real, M., Sansonetty, F., Ludovico, P., Prudêncio, C., Rodrigues, F., Fortuna, M., Sousa, M. J., Silva, M.T. e Leão, C. (2002). "Contributos da citologia analítica para estudos de biologia de leveduras" Boletim de Biotecnologia, **71**: 19-33.

Cuff, M., J. Dyer, et al. (2005). "The human colonic monocarboxylate transporter Isoform 1: its potential importance to colonic tissue homeostasis." Gastroenterology **128**(3): 676-86.

Cuff, M. A., D. W. Lambert, et al. (2002). "Substrate-induced regulation of the human colonic monocarboxylate transporter, MCT1." J Physiol **539**(Pt 2): 361-71.

Dang, C. V., J. W. Kim, et al. (2008). "The interplay between MYC and HIF in cancer." Nat Rev Cancer **8**(1): 51-6.

Dell'Antone, P. (2006). "Inactivation of H+-vacuolar ATPase by the energy blocker 3-bromopyruvate, a new antitumour agent." Life Sci **79**(21): 2049-55.

Devi, M. A. and N. P. Das (1993). "In vitro effects of natural plant polyphenols on the proliferation of normal and abnormal human lymphocytes and their secretions of interleukin-2." Cancer Lett **69**(3): 191-6.

Dimmer, K. S., B. Friedrich, et al. (2000). "The low-affinity monocarboxylate transporter MCT4 is adapted to the export of lactate in highly glycolytic cells." Biochem J **350 Pt 1**: 219-27.

Donohoe, D. R., L. B. Collins, et al. (2012). "The Warburg effect dictates the mechanism of butyrate-mediated histone acetylation and cell proliferation." Mol Cell **48**(4): 612-26.

Donohoe, D. R., K. P. Curry, et al. (2013). "Microbial oncotarget: bacterial-produced butyrate, chemoprevention and Warburg effect." Oncotarget **4**(2): 182-3.

Edinger, A. L. and C. B. Thompson (2002). "Akt maintains cell size and survival by increasing mTOR-dependent nutrient uptake." Mol Biol Cell **13**(7): 2276-88.

El Sayed, S. M., R. M. El-Magd, et al. (2012). "3-Bromopyruvate antagonizes effects of lactate and pyruvate, synergizes with citrate and exerts novel anti-glioma effects." J Bioenerg Biomembr **44**(1): 61-79.

Enerson, B. E. and L. R. Drewes (2003). "Molecular features, regulation, and function of monocarboxylate transporters: implications for drug delivery." J Pharm Sci **92**(8): 1531-44.

Enoki, T., Y. Yoshida, et al. (2006). "Testosterone increases lactate transport, monocarboxylate transporter (MCT) 1 and MCT4 in rat skeletal muscle." J Physiol **577**(Pt 1): 433-43.

Ewald, B., D. Sampath, et al. (2008). "Nucleoside analogs: molecular mechanisms signaling cell death." Oncogene **27**(50): 6522-37.

Fischer, K., P. Hoffmann, et al. (2007). "Inhibitory effect of tumor cell-derived lactic acid on human T cells." Blood **109**(9): 3812-9.

Fleming, S. E., M. D. Fitch, et al. (1991). "Nutrient utilization by cells isolated from rat jejunum, cecum and colon." J Nutr **121**(6): 869-78.

Frauwirth, K. A. and C. B. Thompson (2004). "Regulation of T lymphocyte metabolism." J Immunol **172**(8): 4661-5.

Frisch, S. M. and R. A. Screaton (2001). "Anoikis mechanisms." Curr Opin Cell Biol **13**(5): 555-62.

Gallagher, S. M., J. J. Castorino, et al. (2007). "Monocarboxylate transporter 4 regulates maturation and trafficking of CD147 to the plasma membrane in the metastatic breast cancer cell line MDA-MB-231." Cancer Res **67**(9): 4182-9.

Ganapathy-Kanniappan, S., J. F. Geschwind, et al. (2010). "3-Bromopyruvate induces endoplasmic reticulum stress, overcomes autophagy and causes apoptosis in human HCC cell lines." Anticancer Res **30**(3): 923-35.

Ganapathy-Kanniappan, S., J. F. Geschwind, et al. (2010). "The pyruvic acid analog 3-bromopyruvate interferes with the tetrazolium reagent MTS in the evaluation of cytotoxicity." Assay Drug Dev Technol **8**(2): 258-62.

Ganapathy-Kanniappan, S., J. F. Geschwind, et al. (2009). "Glyceraldehyde-3-phosphate dehydrogenase (GAPDH) is pyruvylated during 3-bromopyruvate mediated cancer cell death." Anticancer Res **29**(12): 4909-18.

Ganapathy-Kanniappan, S., M. Vali, et al. (2010). "3-bromopyruvate: a new targeted antiglycolytic agent and a promise for cancer therapy." Curr Pharm Biotechnol **11**(5): 510-7.

Ganapathy, V., M. Thangaraju, et al. (2008). "Sodium-coupled monocarboxylate transporters in normal tissues and in cancer." AAPS J **10**(1): 193-9.

Gatenby, R. A. and R. J. Gillies (2004). "Why do cancers have high aerobic glycolysis?" Nat Rev Cancer **4**(11): 891-9.

Geschwind, J. F., Y. H. Ko, et al. (2002). "Novel therapy for liver cancer: direct intraarterial injection of a potent inhibitor of ATP production." Cancer Res **62**(14): 3909-13.

Gogvadze, V., B. Zhivotovsky, et al. (2010). "The Warburg effect and mitochondrial stability in cancer cells." Mol Aspects Med **31**(1): 60-74.

Gottschalk, S., N. Anderson, et al. (2004). "Imatinib (STI571)-mediated changes in glucose metabolism in human leukemia BCR-ABL-positive cells." Clin Cancer Res **10**(19): 6661-8.

Gupta, N., P. M. Martin, et al. (2006). "SLC5A8 (SMCT1)-mediated transport of butyrate forms the basis for the tumor suppressive function of the transporter." Life Sci **78**(21): 2419-25.

Halestrap, A. P. (1976). "Transport of pyruvate nad lactate into human erythrocytes. Evidence for the involvement of the chloride carrier and a chloride-independent carrier." Biochem J **156**(2): 193-207.

Halestrap, A. P. (2012). "The monocarboxylate transporter family–Structure and functional characterization." IUBMB Life **64**(1): 1-9.

Halestrap, A. P. and D. Meredith (2004). "The SLC16 gene family-from monocarboxylate transporters (MCTs) to aromatic amino acid transporters and beyond." Pflugers Arch **447**(5): 619-28.

Halestrap, A. P. and N. T. Price (1999). "The proton-linked monocarboxylate transporter (MCT) family: structure, function and regulation." Biochem J **343 Pt 2**: 281-99.

Halestrap, A. P. and M. C. Wilson (2012). "The monocarboxylate transporter family–role and regulation." IUBMB Life **64**(2): 109-19.

Hamer, H. M., D. Jonkers, et al. (2008). "Review article: the role of butyrate on colonic function." Aliment Pharmacol Ther **27**(2): 104-19.

Hanahan, D. and R. A. Weinberg (2000). "The hallmarks of cancer." Cell **100**(1): 57-70.

Hanahan, D. and R. A. Weinberg (2011). "Hallmarks of cancer: the next generation." Cell **144**(5): 646-74.

Hashimoto, T., R. Hussien, et al. (2007). "Lactate sensitive transcription factor network in L6 cells: activation of MCT1 and mitochondrial biogenesis." FASEB J **21**(10): 2602-12.

Hinnebusch, B. F., S. Meng, et al. (2002). "The effects of short-chain fatty acids on human colon cancer cell phenotype are associated with histone hyperacetylation." J Nutr **132**(5): 1012-7.

Hirschhaeuser, F., U. G. Sattler, et al. (2011). "Lactate: a metabolic key player in cancer." Cancer Res **71**(22): 6921-5.

Huang, J., C. Plass, et al. (2011). "Cancer chemoprevention by targeting the epigenome." Curr Drug Targets **12**(13): 1925-56.

Hudis, C. A. and L. Gianni (2011). "Triple-negative breast cancer: an unmet medical need." Oncologist **16 Suppl 1**: 1-11.

Hussien, R. and G. A. Brooks (2011). "Mitochondrial and plasma membrane lactate transporter and lactate dehydrogenase isoform expression in breast cancer cell lines." Physiol Genomics **43**(5): 255-64.

Ihrlund, L. S., E. Hernlund, et al. (2008). "3-Bromopyruvate as inhibitor of tumour cell energy metabolism and chemopotentiator of platinum drugs." Mol Oncol **2**(1): 94-101.

Inan, M. S., R. J. Rasoulpour, et al. (2000). "The luminal short-chain fatty acid butyrate modulates NF-kappaB activity in a human colonic epithelial cell line." Gastroenterology **118**(4): 724-34.

Jardim-Messeder, D., J. Camacho-Pereira, et al. (2012). "3-Bromopyruvate inhibits calcium uptake by sarcoplasmic reticulum vesicles but not SERCA ATP hydrolysis activity." Int J Biochem Cell Biol **44**(5): 801-7.

Jemal, A., F. Bray, et al. (2011). "Global cancer statistics." CA Cancer J Clin **61**(2): 69-90.

Jemal, A., M. M. Center, et al. (2010). "Global patterns of cancer incidence and mortality rates and trends." Cancer Epidemiol Biomarkers Prev **19**(8): 1893-907.

Jones, R. G. and C. B. Thompson (2009). "Tumor suppressors and cell metabolism: a recipe for cancer growth." Genes Dev **23**(5): 537-48.

Juel, C. and A. P. Halestrap (1999). "Lactate transport in skeletal muscle - role and regulation of the monocarboxylate transporter." J Physiol **517 (Pt 3)**: 633-42.

Kawamata, K., H. Hayashi, et al. (2007). "Propionate absorption associated with bicarbonate secretion in vitro in the mouse cecum." Pflugers Arch **454**(2): 253-62.

Kennedy, K. M. and M. W. Dewhirst (2010). "Tumor metabolism of lactate: the influence and therapeutic potential for MCT and CD147 regulation." Future Oncol **6**(1): 127-48.

Kim, J. S., K. J. Ahn, et al. (2008). "Role of reactive oxygen species-mediated mitochondrial dysregulation in 3-bromopyruvate induced cell death in hepatoma cells : ROS-mediated cell death by 3-BrPA." J Bioenerg Biomembr **40**(6): 607-18.

King, M. C., J. H. Marks, et al. (2003). "Breast and ovarian cancer risks due to inherited mutations in BRCA1 and BRCA2." Science **302**(5645): 643-6.

Kirk, P., M. C. Wilson, et al. (2000). "CD147 is tightly associated with lactate transporters MCT1 and MCT4 and facilitates their cell surface expression." EMBO J **19**(15): 3896-904.

Ko, Y. H., P. L. Pedersen, et al. (2001). "Glucose catabolism in the rabbit VX2 tumor model for liver cancer: characterization and targeting hexokinase." Cancer Lett **173**(1): 83-91.

Ko, Y. H., B. L. Smith, et al. (2004). "Advanced cancers: eradication in all cases using 3-bromopyruvate therapy to deplete ATP." Biochem Biophys Res Commun **324**(1): 269-75.

Ko, Y. H., H. A. Verhoeven, et al. (2012). "A translational study "case report" on the small molecule "energy blocker" 3-bromopyruvate (3BP) as a potent anticancer agent: from bench side to bedside." J Bioenerg Biomembr **44**(1): 163-70.

Koppenol, W. H., P. L. Bounds, et al. (2011). "Otto Warburg's contributions to current concepts of cancer metabolism." Nat Rev Cancer **11**(5): 325-37.

Koprinarova, M., P. Markovska, et al. (2010). "Sodium butyrate enhances the cytotoxic effect of cisplatin by abrogating the cisplatin imposed cell cycle arrest." BMC Mol Biol **11**: 49.

Kroemer, G. and J. Pouyssegur (2008). "Tumor cell metabolism: cancer's Achilles' heel." Cancer Cell **13**(6): 472-82.

Lauricella, M., A. Ciraolo, et al. (2011). "SAHA/TRAIL combination induces detachment and anoikis of MDA-MB231 and MCF-7 breast cancer cells." Biochimie **94**(2): 287-99.

Li, C. (2011). "Specific cell cycle synchronization with butyrate and cell cycle analysis." Methods Mol Biol **761**: 125-36.

Li, H., L. Myeroff, et al. (2003). "SLC5A8, a sodium transporter, is a tumor suppressor gene silenced by methylation in human colon aberrant crypt foci and cancers." Proc Natl Acad Sci U S A **100**(14): 8412-7.

Li, K. K., J. C. Pang, et al. (2009). "miR-124 is frequently down-regulated in medulloblastoma and is a negative regulator of SLC16A1." Hum Pathol **40**(9): 1234-43.

Li, X., M. T. Lewis, et al. (2008). "Intrinsic resistance of tumorigenic breast cancer cells to chemotherapy." J Natl Cancer Inst **100**(9): 672-9.

Lopez-Lazaro, M. (2008). "The warburg effect: why and how do cancer cells activate glycolysis in the presence of oxygen?" Anticancer Agents Med Chem **8**(3): 305-12.

Mathupala, S. P., C. B. Colen, et al. (2007). "Lactate and malignant tumors: a therapeutic target at the end stage of glycolysis." J Bioenerg Biomembr **39**(1): 73-7.

Mathupala, S. P., Y. H. Ko, et al. (2009). "Hexokinase-2 bound to mitochondria: cancer's stygian link to the "Warburg Effect" and a pivotal target for effective therapy." Semin Cancer Biol **19**(1): 17-24.

Mathupala, S. P., P. Parajuli, et al. (2004). "Silencing of monocarboxylate transporters via small interfering ribonucleic acid inhibits glycolysis and induces cell death in malignant glioma: an in vitro study." Neurosurgery **55**(6): 1410-9; discussion 1419.

Matsuyama, S., S. Ohkura, et al. (2009). "Food deprivation induces monocarboxylate transporter 2 expression in the brainstem of female rat." J Reprod Dev **55**(3): 256-61.

McClelland, G. B., S. Khanna, et al. (2003). "Peroxisomal membrane monocarboxylate transporters: evidence for a redox shuttle system?" Biochem Biophys Res Commun **304**(1): 130-5.

Merezhinskaya, N. and W. N. Fishbein (2009). "Monocarboxylate transporters: past, present, and future." Histol Histopathol **24**(2): 243-64.

Miyauchi, S., E. Gopal, et al. (2004). "Functional identification of SLC5A8, a tumor suppressor down-regulated in colon cancer, as a Na(+)-coupled transporter for short-chain fatty acids." J Biol Chem **279**(14): 13293-6.

Morris, M. E. and M. A. Felmlee (2008). "Overview of the proton-coupled MCT (SLC16A) family of transporters: characterization, function and role in the transport of the drug of abuse gamma-hydroxybutyric acid." AAPS J **10**(2): 311-21.

Munoz-Pinedo, C., N. El Mjiyad, et al. (2012). "Cancer metabolism: current perspectives and future directions." Cell Death Dis **3**: e248.

Murray, C. M., R. Hutchinson, et al. (2005). "Monocarboxylate transporter MCT1 is a target for immunosuppression." Nat Chem Biol **1**(7): 371-6.

Nabeshima, K., H. Iwasaki, et al. (2006). "Emmprin (basigin/CD147): matrix metalloproteinase modulator and multifunctional cell recognition molecule that plays a critical role in cancer progression." Pathol Int **56**(7): 359-67.

Nakashima, R. A., P. S. Mangan, et al. (1986). "Hexokinase receptor complex in hepatoma mitochondria: evidence from N,N'-dicyclohexylcarbodiimide-labeling studies for the involvement of the pore-forming protein VDAC." Biochemistry **25**(5): 1015-21.

Nelson, J. A. and R. E. Falk (1993). "The efficacy of phloridzin and phloretin on tumor cell growth." Anticancer Res **13**(6A): 2287-92.

Ovens, M. J., A. J. Davies, et al. (2010). "AR-C155858 is a potent inhibitor of monocarboxylate transporters MCT1 and MCT2 that binds to an intracellular site involving transmembrane helices 7-10." Biochem J **425**(3): 523-30.

Ovens, M. J., C. Manoharan, et al. (2010). "The inhibition of monocarboxylate transporter 2 (MCT2) by AR-C155858 is modulated by the associated ancillary protein." Biochem J **431**(2): 217-25.

Pacheco, A. (2012). "Avaliação da atividade antitumoral do 3-bromopiruvato. Papel dos transportadores de monocarboxilatos (MCTs) no seu mecanismo de ação." Master Thesis, Instituto Superior de Ciências da Saúde Norte, 96 pgs.

Paroder, V., S. R. Spencer, et al. (2006). "Na(+)/monocarboxylate transport (SMCT) protein expression correlates with survival in colon cancer: molecular characterization of SMCT." Proc Natl Acad Sci U S A **103**(19): 7270-5.

Pedersen, P. L. (2007). "The cancer cell's "power plants" as promising therapeutic targets: an overview." J Bioenerg Biomembr **39**(1): 1-12.

Pedersen, P. L. (2007). "Warburg, me and Hexokinase 2: Multiple discoveries of key molecular events underlying one of cancers' most common phenotypes, the "Warburg Effect", i.e., elevated glycolysis in the presence of oxygen." J Bioenerg Biomembr **39**(3): 211-22.

Pedersen, P. L. (2012). "3-Bromopyruvate (3BP) a fast acting, promising, powerful, specific, and effective "small molecule" anti-cancer agent taken from labside to bedside: introduction to a special issue." J Bioenerg Biomembr **44**(1): 1-6.

Pelicano, H., D. S. Martin, et al. (2006). "Glycolysis inhibition for anticancer treatment." Oncogene **25**(34): 4633-46.

Pereira da Silva, A. P., T. El-Bacha, et al. (2009). "Inhibition of energy-producing pathways of HepG2 cells by 3-bromopyruvate." Biochem J **417**(3): 717-26.

Pertega-Gomes, N., J. R. Vizcaino, et al. (2011). "Monocarboxylate transporter 4 (MCT4) and CD147 overexpression is associated with poor prognosis in prostate cancer." BMC Cancer **11**: 312.

Pharoah, P. D., A. M. Dunning, et al. (2004). "Association studies for finding cancer-susceptibility genetic variants." Nat Rev Cancer **4**(11): 850-60.

Philippe, I., Z. Xiao-Dong, et al. (2012). "Experimental results using 3-bromopyruvate in mesothelioma: in vitro and in vivo studies." J Bioenerg Biomembr **44**(1): 81-90.

Philp, N. J., J. D. Ochrietor, et al. (2003). "Loss of MCT1, MCT3, and MCT4 expression in the retinal pigment epithelium and neural retina of the 5A11/basigin-null mouse." Invest Ophthalmol Vis Sci **44**(3): 1305-11.

Pinheiro, C., A. Albergaria, et al. (2010). "Monocarboxylate transporter 1 is up-regulated in basal-like breast carcinoma." Histopathology **56**(7): 860-7.

Pinheiro, C., A. Longatto-Filho, et al. (2012). "Role of monocarboxylate transporters in human cancers: state of the art." J Bioenerg Biomembr **44**(1): 127-39.

Pinheiro, C., A. Longatto-Filho, et al. (2008). "Increasing expression of monocarboxylate transporters 1 and 4 along progression to invasive cervical carcinoma." Int J Gynecol Pathol **27**(4): 568-74.

Pinheiro, C., A. Longatto-Filho, et al. (2008). "Increased expression of monocarboxylate transporters 1, 2, and 4 in colorectal carcinomas." Virchows Arch **452**(2): 139-46.

Pinheiro, C., A. Longatto-Filho, et al. (2009). "The prognostic value of CD147/EMMPRIN is associated with monocarboxylate transporter 1 co-expression in gastric cancer." Eur J Cancer **45**(13): 2418-24.

Pinheiro, C., R. M. Reis, et al. (2010). "Expression of monocarboxylate transporters 1, 2, and 4 in human tumours and their association with CD147 and CD44." J Biomed Biotechnol **2010**: 427694.

Poole, R. C. and A. P. Halestrap (1991). "Reversible and irreversible inhibition, by stilbenedisulphonates, of lactate transport into rat erythrocytes. Identification of some new high-affinity inhibitors." Biochem J **275 (Pt 2)**: 307-12.

Poole, R. C., C. E. Sansom, et al. (1996). "Studies of the membrane topology of the rat erythrocyte H+/lactate cotransporter (MCT1)." Biochem J **320 (Pt 3)**: 817-24.

Pullen, T. J., G. da Silva Xavier, et al. (2011). "miR-29a and miR-29b contribute to pancreatic beta-cell-specific silencing of monocarboxylate transporter 1 (Mct1)." Mol Cell Biol **31**(15): 3182-94.

Queiros, O., A. Preto, et al. (2012). "Butyrate activates the monocarboxylate transporter MCT4 expression in breast cancer cells and enhances the antitumor activity of 3-bromopyruvate." J Bioenerg Biomembr **44**(1): 141-53.

Racker, E. (1974). "History of the Pasteur effect and its pathobiology." Mol Cell Biochem **5**(1-2): 17-23.

Rohwer, N., M. Welzel, et al. (2008). "Hypoxia-inducible factor 1alpha mediates anoikis resistance via suppression of alpha5 integrin." Cancer Res **68**(24): 10113-20.

Schulze, A. and A. L. Harris (2012). "How cancer metabolism is tuned for proliferation and vulnerable to disruption." Nature **491**(7424): 364-73.

Semenza, G. L. (2008). "Tumor metabolism: cancer cells give and take lactate." J Clin Invest **118**(12): 3835-7.

Shim, H., C. Dolde, et al. (1997). "c-Myc transactivation of LDH-A: implications for tumor metabolism and growth." Proc Natl Acad Sci U S A **94**(13): 6658-63.

Shoshan, M. C. (2012). "3-Bromopyruvate: targets and outcomes." J Bioenerg Biomembr **44**(1): 7-15.

Simpson, C. D., K. Anyiwe, et al. (2008). "Anoikis resistance and tumor metastasis." Cancer Lett **272**(2): 177-85.

Slomiany, M. G., G. D. Grass, et al. (2009). "Hyaluronan, CD44, and emmprin regulate lactate efflux and membrane localization of monocarboxylate transporters in human breast carcinoma cells." Cancer Res **69**(4): 1293-301.

Sorlie, T., C. M. Perou, et al. (2001). "Gene expression patterns of breast carcinomas distinguish tumor subclasses with clinical implications." Proc Natl Acad Sci U S A **98**(19): 10869-74.

Sotiriou, C., S. Y. Neo, et al. (2003). "Breast cancer classification and prognosis based on gene expression profiles from a population-based study." Proc Natl Acad Sci U S A **100**(18): 10393-8.

Stern, R., S. Shuster, et al. (2002). "Lactate stimulates fibroblast expression of hyaluronan and CD44: the Warburg effect revisited." Exp Cell Res **276**(1): 24-31.

Stockwin, L. H., S. X. Yu, et al. (2010). "Sodium dichloroacetate selectively targets cells with defects in the mitochondrial ETC." Int J Cancer **127**(11): 2510-9.

Tennant, D. A., R. V. Duran, et al. (2010). "Targeting metabolic transformation for cancer therapy." Nat Rev Cancer **10**(4): 267-77.

Thangaraju, M., G. Cresci, et al. (2008). "Sodium-coupled transport of the short chain fatty acid butyrate by SLC5A8 and its relevance to colon cancer." J Gastrointest Surg **12**(10): 1773-81.

Thangaraju, M., S. K. Karunakaran, et al. (2009). "Transport by SLC5A8 with subsequent inhibition of histone deacetylase 1 (HDAC1) and HDAC3 underlies the antitumor activity of 3-bromopyruvate." Cancer **115**(20): 4655-66.

Ullah, M. S., A. J. Davies, et al. (2006). "The plasma membrane lactate transporter MCT4, but not MCT1, is up-regulated by hypoxia through a HIF-1alpha-dependent mechanism." J Biol Chem **281**(14): 9030-7.

Vander Heiden, M. G., L. C. Cantley, et al. (2009). "Understanding the Warburg effect: the metabolic requirements of cell proliferation." Science **324**(5930): 1029-33.

Velazquez, O. C., H. M. Lederer, et al. (1997). "Butyrate and the colonocyte. Production, absorption, metabolism, and therapeutic implications." Adv Exp Med Biol **427**: 123-34.

Visvader, J. E. (2009). "Keeping abreast of the mammary epithelial hierarchy and breast tumorigenesis." Genes Dev **23**(22): 2563-77.

Vogelstein, B. and K. W. Kinzler (2004). "Cancer genes and the pathways they control." Nat Med **10**(8): 789-99.

Vossen, J. A., M. Buijs, et al. (2008). "Development of a new orthotopic animal model of metastatic liver cancer in the rabbit VX2 model: effect on metastases after partial hepatectomy, intra-arterial treatment with 3-bromopyruvate and chemoembolization." Clin Exp Metastasis **25**(7): 811-7.

Warburg, O. (1956). "On the origin of cancer cells." Science **123**(3191): 309-14.

Wilson, J. E. (1995). "Hexokinases." Rev Physiol Biochem Pharmacol **126**: 65-198.

Wilson, J. E. (1997). "An introduction to the isoenzymes of mammalian hexokinase types I-III." Biochem Soc Trans **25**(1): 103-7.

Wise, D. R., R. J. DeBerardinis, et al. (2008). "Myc regulates a transcriptional program that stimulates mitochondrial glutaminolysis and leads to glutamine addiction." Proc Natl Acad Sci U S A **105**(48): 18782-7.

Xu, R. H., H. Pelicano, et al. (2005). "Synergistic effect of targeting mTOR by rapamycin and depleting ATP by inhibition of glycolysis in lymphoma and leukemia cells." Leukemia **19**(12): 2153-8.

Zhang, Q., J. Pan, et al. (2012). "Aerosolized 3-bromopyruvate inhibits lung tumorigenesis without causing liver toxicity." Cancer Prev Res (Phila) **5**(5): 717-25.